https://ntrs.nasa.gov/search.jsp?R=19930090513 2020-06-17T04:24:24+00:00Z

NACA RM E54J07

NACA

RESEARCH MEMORANDUM

COMPARISON AT SUPERSONIC SPEEDS OF TRANSLATING SPIKE INLETS HAVING BLUNT- AND SHARP-LIP COWLS

By Gerald C. Gorton and Murray Dryer

Lewis Flight Propulsion Laboratory
Cleveland, Ohio

NATIONAL ADVISORY COMMITTEE
FOR AERONAUTICS

WASHINGTON

January 19, 1955
Declassified October 31, 1958

ERRATA

NACA RM E54J07

COMPARISON AT SUPERSONIC SPEEDS OF TRANSLATING SPIKE INLETS HAVING BLUNT- AND SHARP-LIP COWLS

By Gerald C. Gorton and Murray Dryer

January 19, 1955

The page on the reverse side of this sheet should be inserted in place of the present page 15.

3497

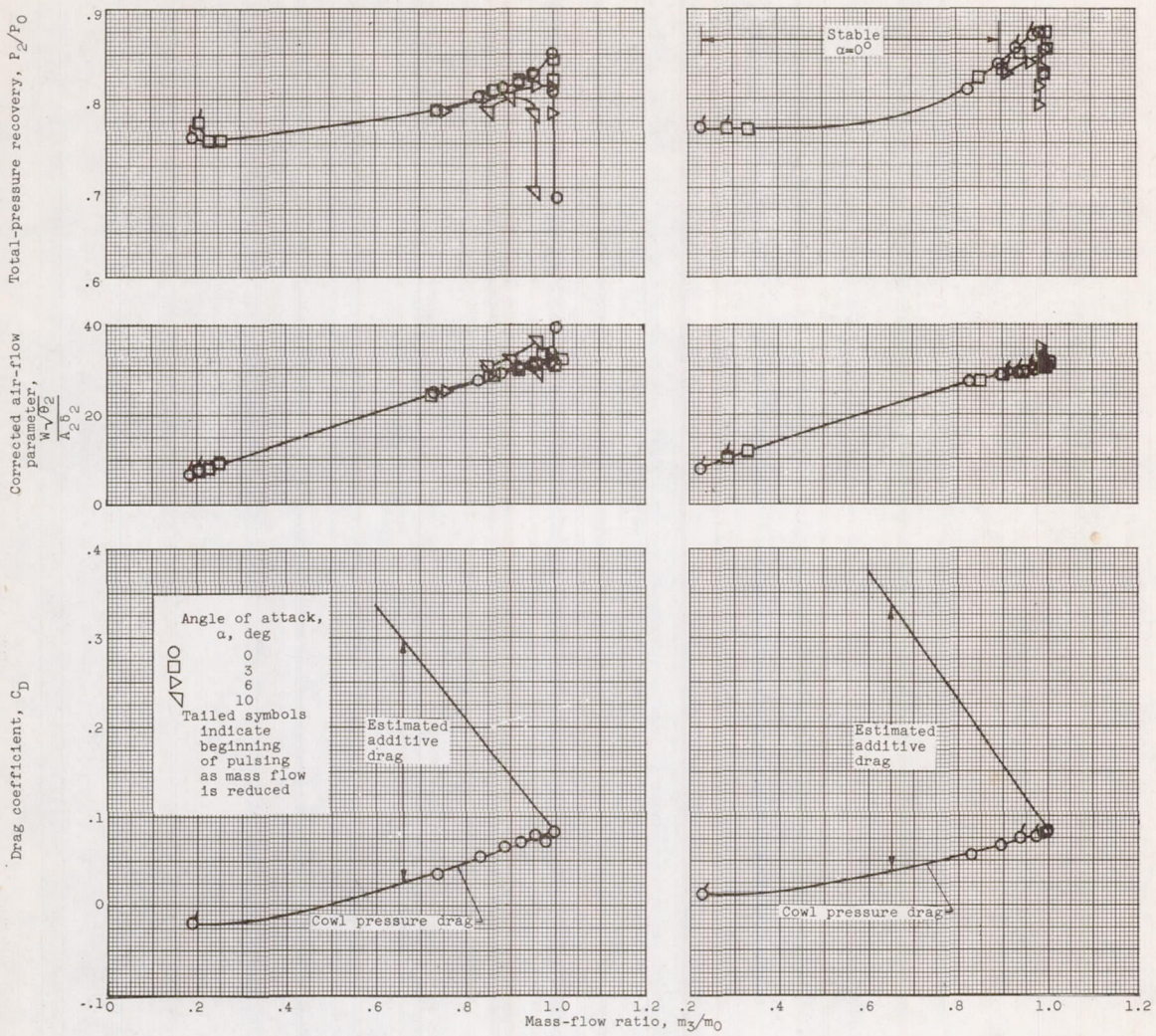

(c) Cowl-position parameter, θ_l, 44.3°.

(d) Cowl-position parameter, θ_l, 43.3°.

Figure 3. - Continued. Performance of sharp-lip inlet at a free-stream Mach number of 2.0. Shock angle, 43.0°.

NATIONAL ADVISORY COMMITTEE FOR AERONAUTICS

RESEARCH MEMORANDUM

COMPARISON AT SUPERSONIC SPEEDS OF TRANSLATING SPIKE INLETS HAVING BLUNT- AND SHARP-LIP COWLS

By Gerald C. Gorton and Murray Dryer

3497

CG-1

SUMMARY

Two translating spike inlets having blunt- and sharp-lip cowls were investigated in the Lewis 8- by 6-foot supersonic wind tunnel at free-stream Mach numbers of 1.5, 1.8, and 2.0 and at angles of attack from 0° to 10°.

Pressure recoveries on the order of 0.90 were obtained with both inlets at Mach number 2.0 for cowl-position parameters causing the oblique shock to fall ahead of the cowl lip. On a thrust-minus-drag basis, the choice of inlet would depend on the criterion used for inlet-engine matching as well as the air-flow schedule of the particular engine considered.

Comparable stable mass-flow ranges were obtained (stable for mass-flow ratios greater than approx. 0.20) with both inlets when the spike was positioned to cause the oblique shock to fall within the inlet. However, for spike positions causing the oblique shock to fall outside the lip at Mach numbers 1.8 and 2.0, the blunt lip generally had the greater stable range.

INTRODUCTION

A supersonic airplane designed to fly over a wide range of Mach numbers generally requires some form of variable inlet geometry in order to obtain optimum propulsion-system performance. For nose or nacelle inlet installations, there are many inherent advantages in using a translating spike as the variable geometry feature. Investigations of the operating problems of such inlets up to a design Mach number of 2.0 are reported in references 1 to 3. These studies have shown that, if cowl-lip angles are made low to minimize cowl pressure drag, there will either be excessive internal contraction or external flow expansion on the spike for part of the range of operation. The contraction causes additive drag, and the expansion reduces pressure recovery (refs. 1 and 2). These

undesirable internal flow characteristics can be avoided by using larger cowl-lip angles (ref. 3).

This report presents the results of an investigation of translating-spike inlets designed to avoid the flow expansion ahead of the cowl lip but with a compromise lip angle which results in some internal contraction as the spike is translated. Two cowls, consisting of a blunt and a sharp lip, were investigated.

The investigation was conducted in the NACA Lewis 8- by 6-foot supersonic wind tunnel. The study included an evaluation of the pressure recovery and stability of the inlets over a wide range of mass flows at Mach numbers from 1.5 to 2.0 and angles of attack from 0° to 10°. Cowl pressure drags were determined from pressure distributions at zero angle of attack.

SYMBOLS

The following symbols are used in this report:

A	flow area, sq ft
A_M	maximum cross-sectional area, 0.534 sq ft
A_0	inlet capture area (blunt-lip inlet, 0.294 sq ft; sharp-lip inlet, 0.257 sq ft)
C_D	drag-coefficient, D/q_0A_M
D	drag, lb
F	thrust with measured total-pressure recovery, lb
F_i	thrust with 100 percent total-pressure recovery, lb
M	Mach number
m	mass flow, slugs/sec
m_0	mass flow through a stream tube defined by inlet capture area A_0, slugs/sec
P	total pressure, lb/sq ft
p	static pressure, lb/sq ft
q	dynamic pressure, $\gamma pM^2/2$, lb/sq ft

3497 CG-1 back

$\frac{W\sqrt{\theta}}{\delta A}$	corrected air-flow parameter, lb/sec/sq ft
W	weight flow, lb/sec
x	axial distance from cowl lip, in.
α	angle of attack, deg
γ	ratio of specific heats for air, 1.4
δ	total pressure divided by NACA standard sea-level static pressure
θ	stream total temperature divided by NACA standard sea-level static temperature
θ_l	cowl-position parameter (angle between axis of diffuser and line joining apex of cone to cowl lip), deg
φ	theoretical oblique shock angle, deg

Subscripts:

0	free stream
2	diffuser exit
3	air-flow measuring station

APPARATUS AND PROCEDURE

The inlet model was supported below the tunnel centerline by a strut-supported sting (fig. 1(a)). Geometric details of the sharp-lip and blunt-lip cowls are shown in figures 1(b) and (c), respectively. Coordinates of both cowls are referenced to a common axial station ($x = 0$) located upstream of the lip. All coordinates downstream of $x = 2.688$ are identical for both cowls. The blunt-lip cowl had a larger capture area, hence less projected frontal area than the sharp-lip cowl.

Details of the centerbody are shown in figure 1(d). The portion of the centerbody that translates was composed of a 50° included-angle conical spike which faired into a cylindrical section. This cylindrical section translated over a fixed cylindrical portion of the centerbody. The diffuser-area variation of both inlets for various positions of the spike is shown in figure 2.

At any flow condition, a Mach number could be determined at station 3 (fig. 1(a)) by assuming one-dimensional isentropic flow to the choked exit area. If Mach number were combined with an average measured static pressure from six orifices at station 3 and the free-stream total temperature, the inlet mass flow could be calculated. The calculated mass flow and the static pressure from eight orifices at station 2 were then used to compute Mach number, total pressure, and corrected air-flow parameter at station 2, the diffuser-discharge station.

Cowl pressure drag at zero angle of attack was obtained from an integration of the static pressures along the cowl. Static-pressure orifices were located on the horizontal plane as shown in figures 1(b) and (c).

A dynamic static-pressure pickup, located slightly downstream of station 2, was used in conjunction with schlieren apparatus to determine the onset of pulsing. The start of pulsing was sufficiently abrupt to allow the determination of the mass-flow ratio at which pulsing first occurred.

DISCUSSION OF RESULTS

The measured performance characteristics for the sharp-lip-inlet model are presented in figures 3 to 5 as a function of mass-flow ratio for various values of cowl-position parameter θ_l. Similar data are presented in figures 6 to 8 for the blunt-lip inlet. At $M_0 = 2$, both inlets exhibited maximum pressure recoveries on the order of 90 percent of free-stream total pressure. These maximum values occurred at cowl-position parameters, which were less than the theoretical oblique shock angle $\varphi = 43^\circ$.

Included on these figures are the cowl pressure drags at zero angle of attack and the estimated additive drags. The additive drags were approximated by a linear variation between the minimum value predicted in reference 4 for each critical mass-flow ratio and a value corresponding to the stagnation condition at zero mass-flow ratio.

Inlet stability. - Mass-flow ratios at which each configuration became unstable are indicated on figures 3 to 8. For the sharp-lip inlet at spike positions corresponding to $\theta_l = 43.3^\circ$ and 42.1°, a region of instability was encountered at $M_0 = 2.0$ near the critical mass-flow ratio (fig. 5). As the mass flow was reduced the flow became stable and remained so to a very low value of mass-flow ratio.

The stability characteristics are summarized on figure 9 for zero angle of attack. The mass-flow ratio at which instability was noted is plotted as a function of cowl-position parameter θ_l. The value of

cowl-position parameter for which the oblique shock would intersect the cowl lip in the absence of internal choking is indicated for each flight speed ($\theta_l = \varphi$).

The inlets had comparable regions of stability (stable for mass-flow ratios greater than approx. 0.20) at Mach number 1.5 and at higher Mach numbers for spike projections causing the oblique shock to fall inside the cowl lip ($\theta_l > \varphi$). At Mach numbers 1.8 and 2.0, the stable range decreased as the spike was extended to cause the oblique shock to fall ahead of the inlet ($\theta_l < \varphi$). The decrease was gradual except for the sharp-lip inlet at Mach number 2.0 where the previously noted intermittent unstability occurred. At Mach numbers 1.8 and 2.0 and at $\theta_l < \varphi$, the blunt-lip inlet generally had the larger stable mass-flow range.

Critical inlet performance, zero angle of attack. - A summary of inlet characteristics at critical operation is shown in figure 10 for zero angle of attack. There was a pronounced decrease in the critical pressure recovery with both inlets at Mach number 2.0 as the spike was retracted. This effect was less pronounced at lower Mach number. The reduction was primarily associated with the changes in the relative amount of air that was captured by the inlet and passed through both the oblique and normal shocks. Changes in the shock structure resulted from the oblique shock movement caused by spike translation and the normal shock movement ahead of the inlet because of excessive internal contraction (see schlieren photographs of fig. 11).

The cowl pressure-drag coefficients for critical operation were essentially independent of spike translation. However, as a result of leading-edge suction, lower cowl-lip angle, and less projected frontal area, the cowl pressure-drag coefficients for the blunt-lip inlet were considerably less than those for the sharp-lip inlets. At $M_0 = 1.5$, for example, the leading-edge suction was sufficient to constitute a thrust force on the blunt-lip inlet.

Also shown in figure 10 are curves of cowl pressure plus estimated additive drag coefficient. For most conditions, even though the cowl pressure drag was lower for the blunt-lip inlet, the additive drag was sufficiently greater to result in higher over-all drags at critical inlet conditions. However, for forward spike positions ($\theta_l < 41.0^\circ$) at $M_0 = 2.0$, the additive drag was reduced to the point where the lower cowl pressure drag of the blunt lip became a more appreciable part of the over-all drag. As a result, the over-all drag coefficient was less for the blunt-lip inlet than for the sharp-lip inlet.

Inlet-engine matching. - A thrust-minus-drag comparison of the blunt- and sharp-lip inlets and the inlet of reference 3 was made by matching the inlets to several turbojet engines. In order to make the data of reference 3 comparable with the present investigation, the friction drag

of the model for reference 3 was subtracted from its total drag. The air-flow schedules for the engines are shown in figure 12. The criterion used for matching was that each inlet would be sized for optimum performance at Mach number 2.0 and that the spike would be translated to obtain optimum performance at the lower Mach numbers of 1.8 and 1.5. The effective thrust parameter $\frac{F - D}{F_i}$ used for the comparison was calculated according to the method of reference 5, assuming the engines operate with maximum afterburning in the tropopause. The results of these calculations are presented in figure 13.

The blunt-lip inlet was superior on an effective-thrust-parameter basis at Mach number 2.0 to both the sharp-lip inlet and the inlet of reference 3. At lower Mach numbers, however, the blunt-lip inlet was either comparable or inferior in performance.

The air-flow requirements of each engine determined the amount of spike translation necessary to obtain the most efficient inlet-engine matching (fig. 14). Engine C required the largest amount of spike translation ($\Delta\theta_l \approx 12^\circ$), since its required air-flow variation (fig. 12) for the Mach number range 1.5 to 2.0 was greater than for engines A and B. It is for such large translations that an inlet with no internal contraction may show advantage. An illustration of this advantage is the matching of engine C to the three inlets at Mach number 1.5. Only the inlet of reference 3, which did not have internal contraction, allowed matching at a high pressure-recovery condition. The sharp-lip and blunt-lip inlets incorporated enough internal contraction to cause a normal shock to position itself ahead of the inlet, thus spilling mass flow in excess of that which would allow efficient matching.

It is apparent that the choice of inlet for a given engine is dependent, not only on the criterion used in matching, but also on the air-flow schedule of the particular engine.

SUMMARY OF RESULTS

The following observations were made from an experimental investigation at Mach numbers 1.5, 1.8, and 2.0 of a blunt-lip and a sharp-lip inlet equipped with a translating-spike centerbody:

1. Pressure recoveries on the order of 0.90 were obtained by both the sharp-lip and blunt-lip inlet at Mach number 2.0 for cowl-position parameters less than the theoretical oblique shock angle ($\theta_l < 43^\circ$).

2. On a thrust-minus-drag basis, the choice of inlet depends on the criterion selected for inlet-engine matching as well as the required air-flow schedule of the particular engine considered.

3. Both inlets were stable down to mass-flow ratios of approximately 0.20 when the spike was positioned to cause the oblique shock to fall within the inlet ($\theta_l > \varphi$). However, at Mach numbers 1.8 and 2.0 for spike positions causing the oblique shock to fall outside the cowl lip ($\theta_l < \varphi$), the blunt-lip inlet generally had the larger stable range.

Lewis Flight Propulsion Laboratory
National Advisory Committee for Aeronautics
Cleveland, Ohio, October 14, 1954

REFERENCES

1. Gorton, Gerald C.: Investigation of Translating-Spike Supersonic Inlet as Means of Mass-Flow Control at Mach Numbers of 1.5, 1.8, and 2.0. NACA RM E53G10, 1953.

2. Leissler, L. Abbott, and Sterbentz, William H.: Investigation of a Translating-Cone Inlet at Mach Numbers from 1.5 to 2.0. NACA RM E54B23, 1954.

3. Gorton, Gerald C.: Investigation at Supersonic Speeds of a Translating-Spike Inlet Employing a Steep-Lip Cowl. NACA RM E54G29, 1954.

4. Sibulkin, Merwin: Theoretical and Experimental Investigation of Additive Drag. NACA RM E51B13, 1951.

5. Kremzier, Emil J.: A Method for Evaluating the Effects of Drag and Inlet Pressure Recovery on Propulsion-System Performance. NACA TN 3261, 1954.

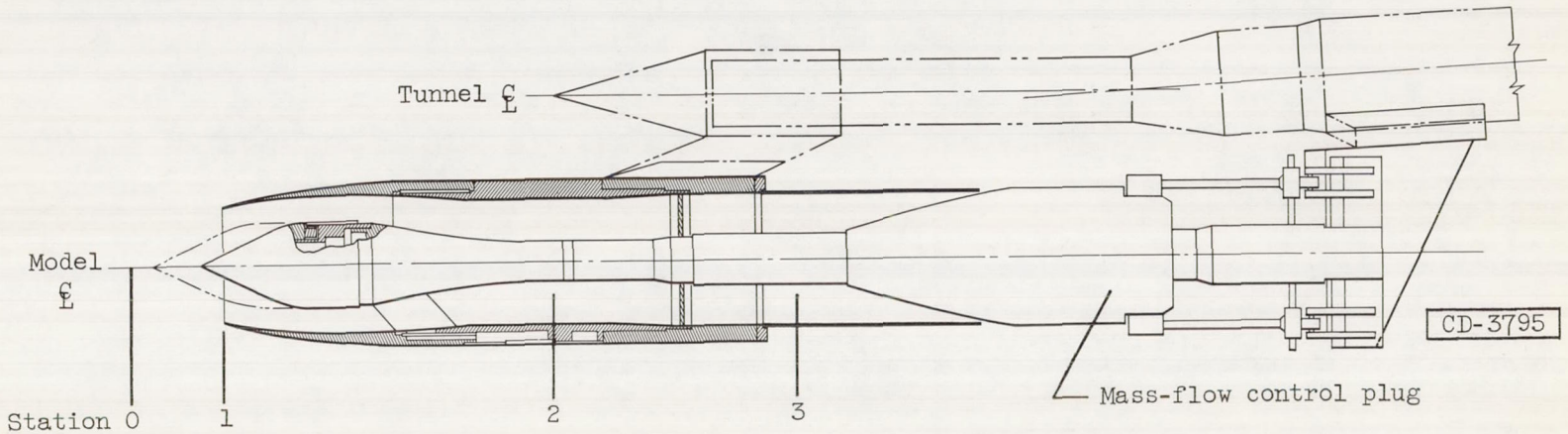

(a) Installation in 8- by 6-foot supersonic wind tunnel.

Figure 1. - Schematic diagrams of translating-spike inlet model.

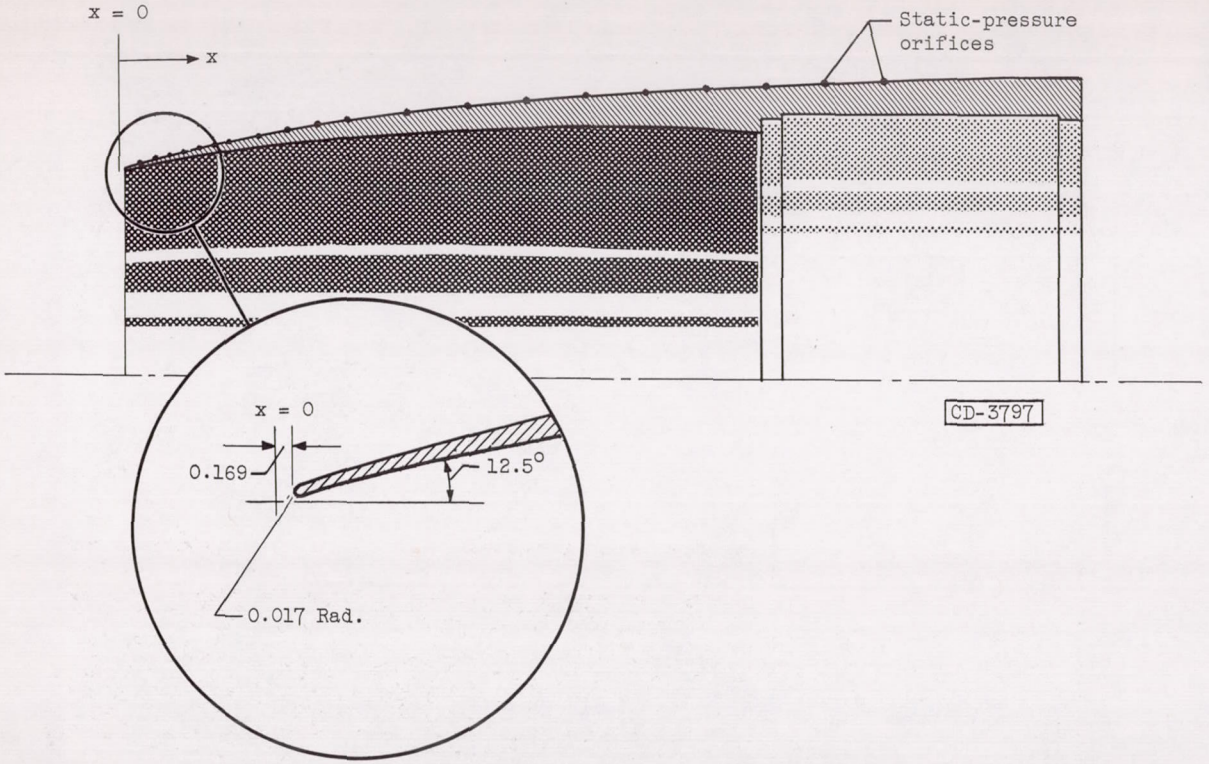

Nacelle coordinates		
Station	Internal radius, in.	External radius, in.
0.188	3.420	3.453
1.438	3.696	3.788
2.688	3.870	4.034
3.938	3.960	4.228
5.188	4.030	4.381
6.438	4.088	4.505
7.688	4.130	4.606
8.938	4.150	4.691
10.188	4.101	4.764
10.880	4.060	4.800
11.438	4.020	4.829
12.688	3.930	4.889
13.938	3.890	4.920
15.188	3.850	4.950
16.250	3.830	↓
17.500	3.808	
18.000	3.805	
18.750	3.800	
20.000	↓	
21.250		

(b) Details of sharp-lip inlet.

Figure 1. - Continued. Schematic diagrams of translating-spike inlet model. (All dimensions in inches.)

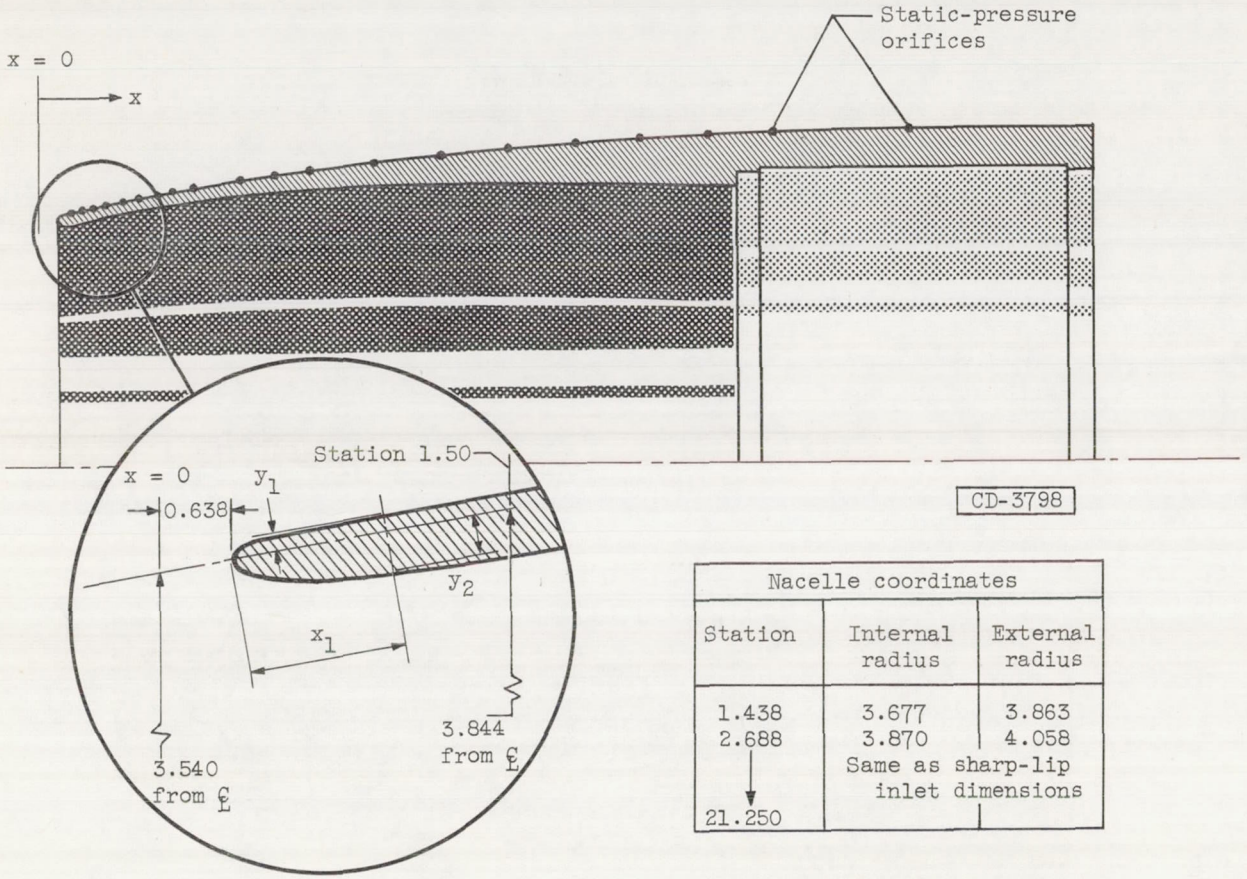

Nacelle coordinates		
Station	Internal radius	External radius
1.438	3.677	3.863
2.688	3.870	4.058
↓	Same as sharp-lip inlet dimensions	
21.250		

Nacelle-lip coordinates		
x_1	y_1	y_2
0	0	0
.013	.016	.030
.025	.023	.040
.038	.029	.049
.050	.033	.056
.063	.037	.063
.075	.040	.069
.100	.044	.080
.125	.047	.090
.150	.049	.100
.180	.050	.108
.200	↓	.113
.225		.119
.250		.123
.313		.134
.375		.141
.438		.146
.500		.150
.540	↓	.150

(c) Details of blunt-lip inlet.

Figure 1. - Continued. Schematic diagrams of translating-spike inlet model. (All dimensions in inches.)

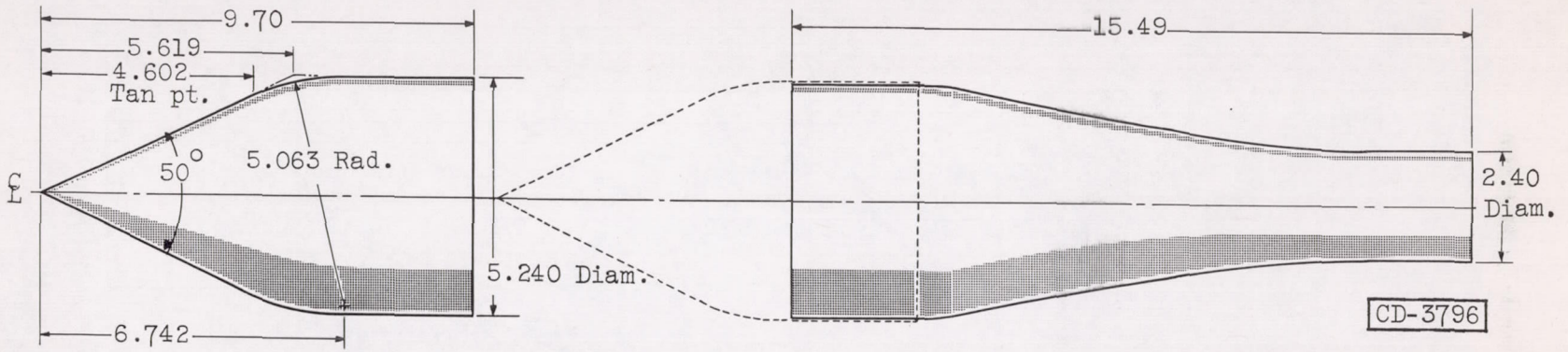

(d) Translating-spike centerbody.

Figure 1. - Concluded. Schematic diagrams of translating-spike inlet model. (All dimensions in inches.)

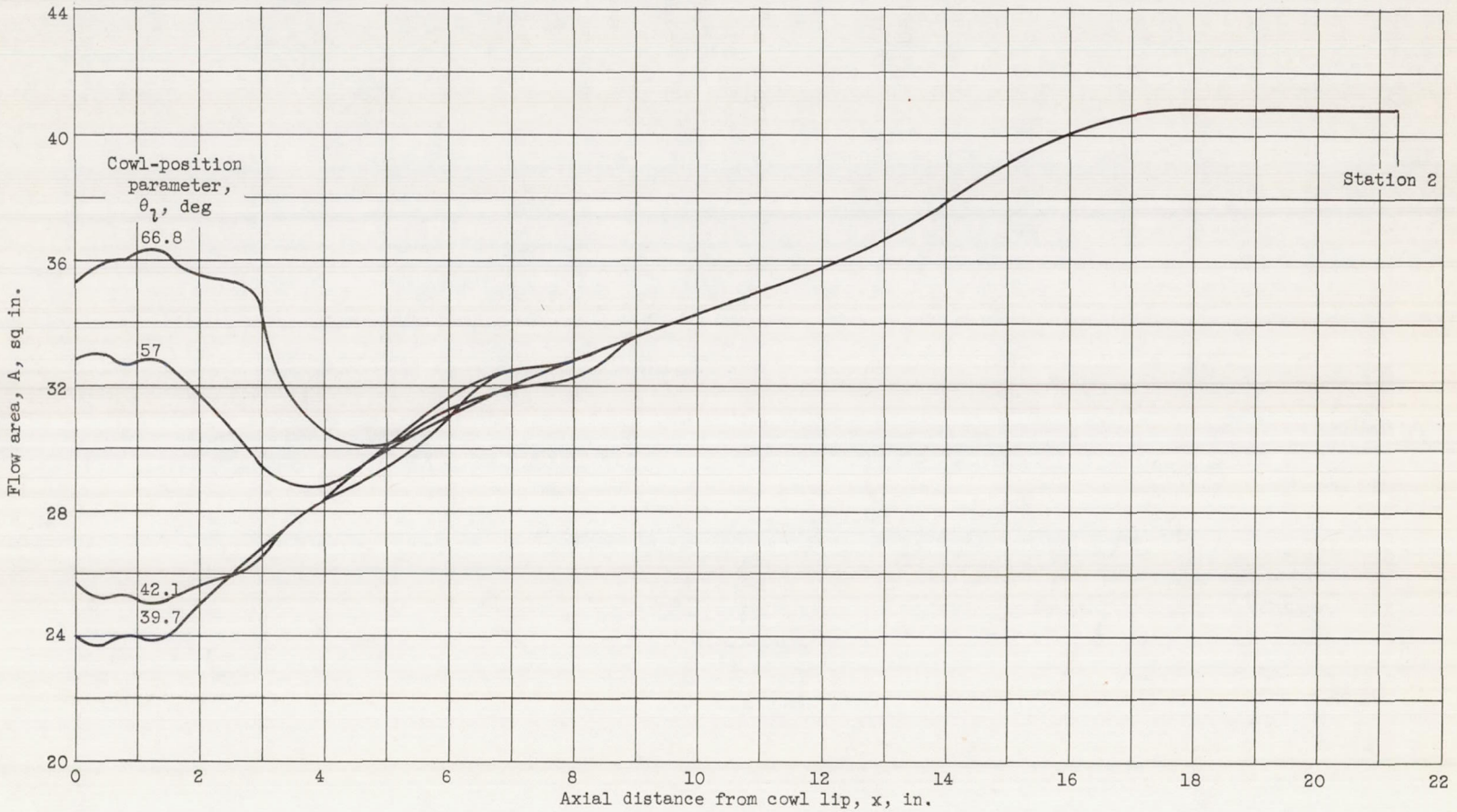

(a) Sharp-lip inlet.

Figure 2. - Diffuser-area variation.

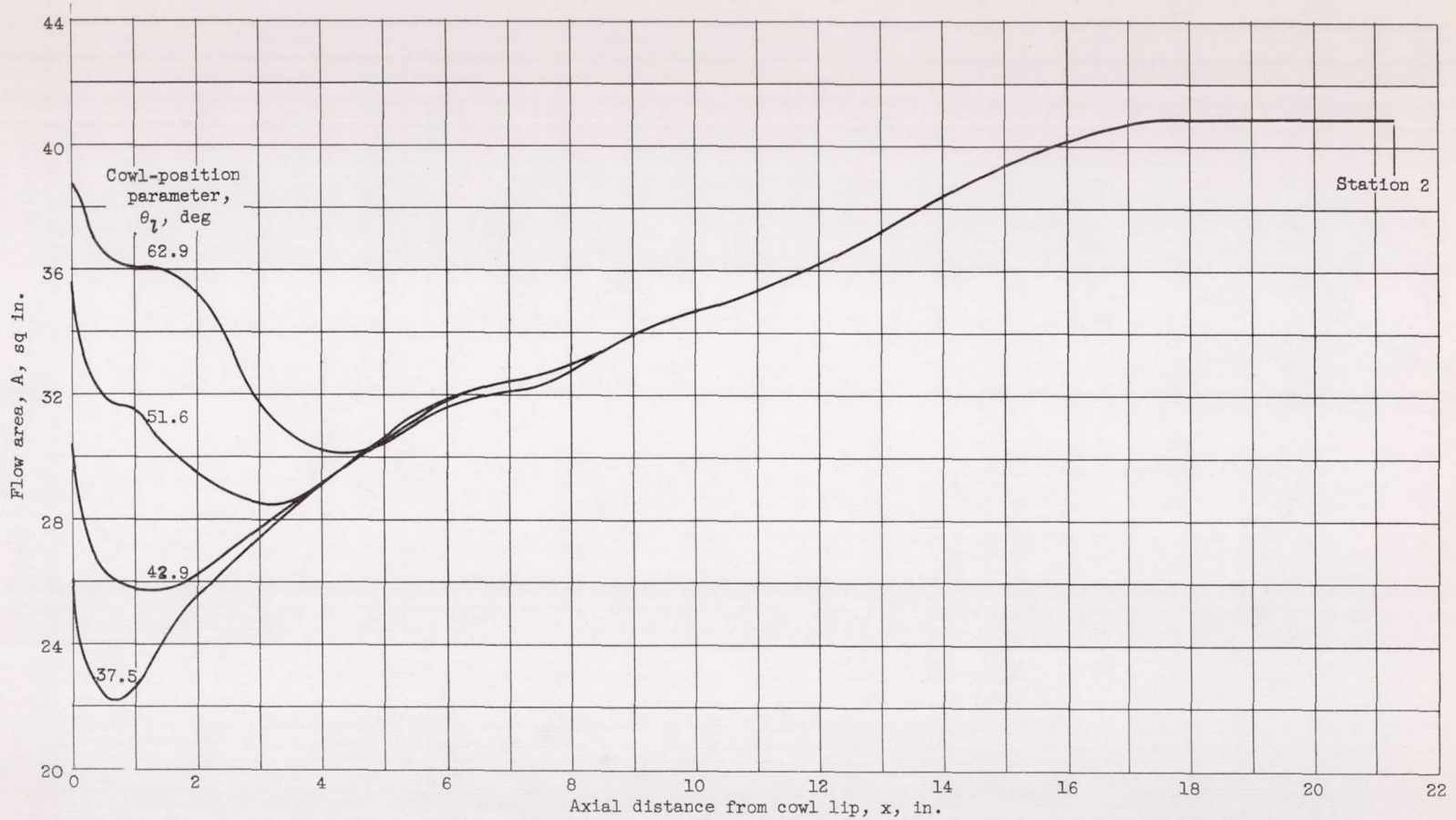

(b) Blunt-lip inlet.

Figure 2. - Concluded. Diffuser-area variation.

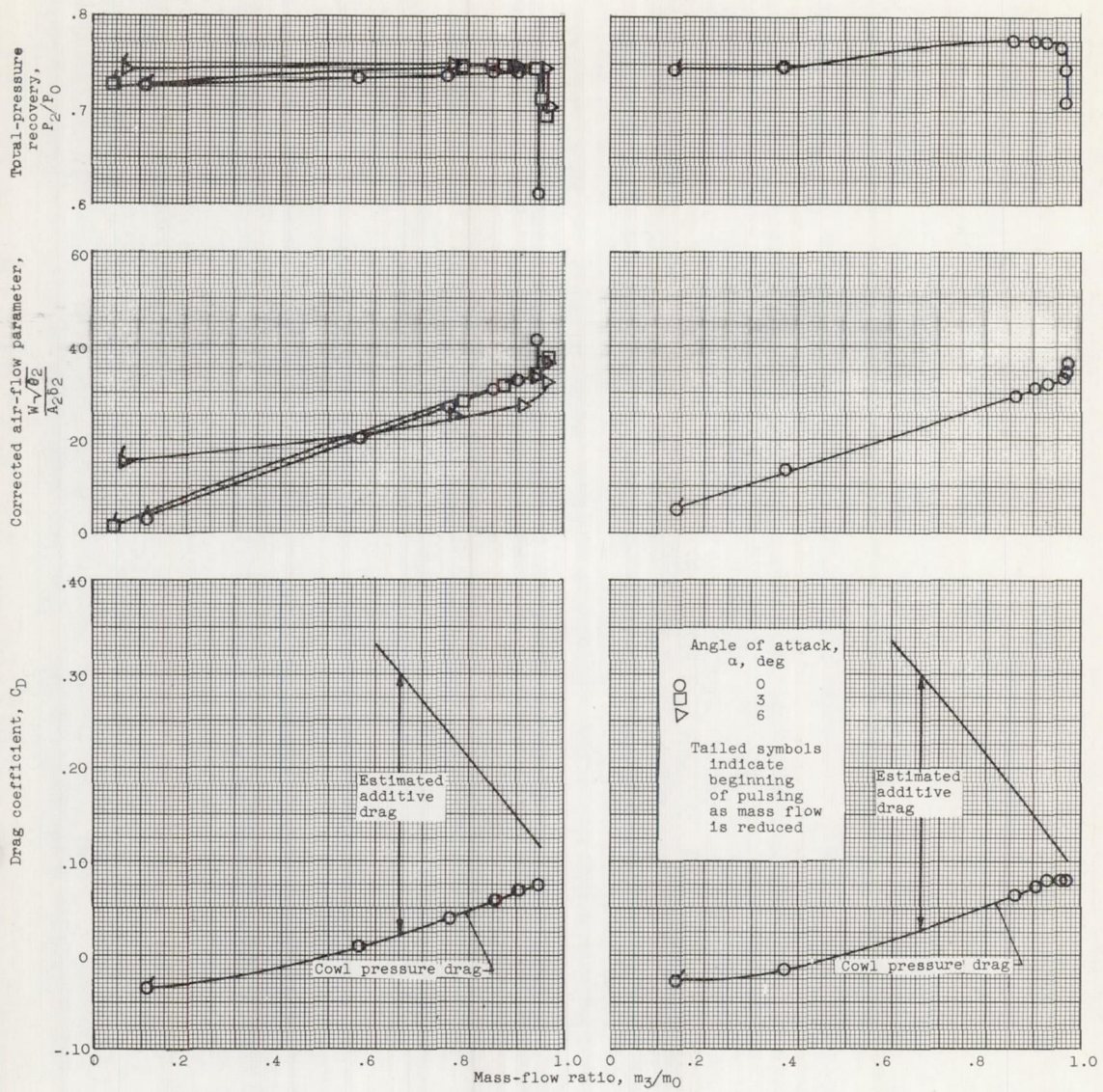

(a) Cowl-position parameter, θ_l, 57°. (b) Cowl-position parameter, θ_l, 46.8.

Figure 3. - Performance of sharp-lip inlet at a free-stream Mach number of 2.0. Shock angle, 43.0°.

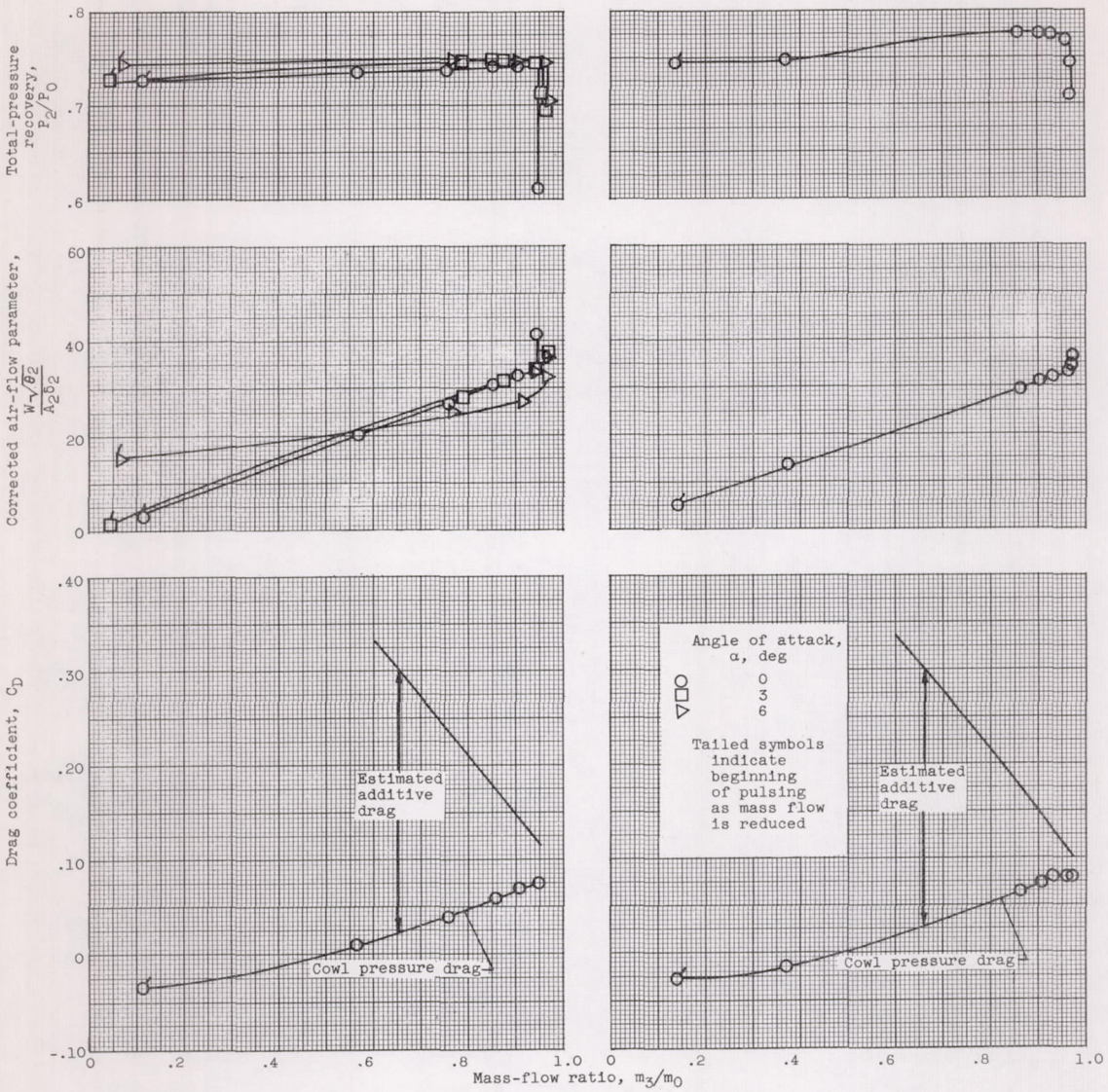

(a) Cowl-position parameter, θ_l, 57°. (b) Cowl-position parameter, θ_l, 46.8.

Figure 3. - Performance of sharp-lip inlet at a free-stream Mach number of 2.0. Shock angle, 43.0°.

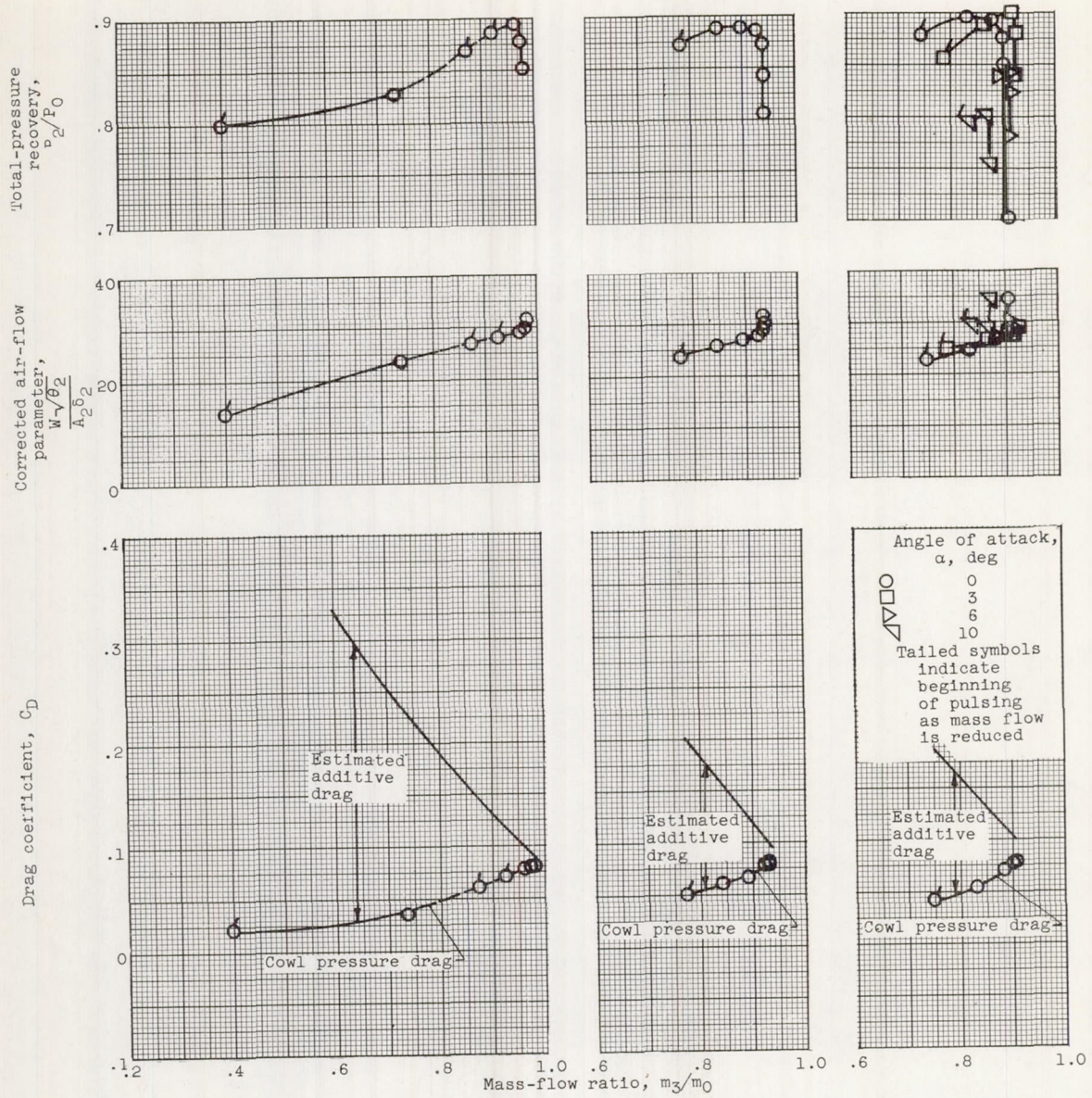

(e) Cowl-position parameter, θ_l, 42.1°.

(f) Cowl-position parameter, θ_l, 40.8°.

(g) Cowl-position parameter, θ_l, 39.7°.

Figure 3. - Concluded. Performance of sharp-lip inlet at a free-stream Mach number of 2.0. Shock angle, 43.0°.

CG-3 3497

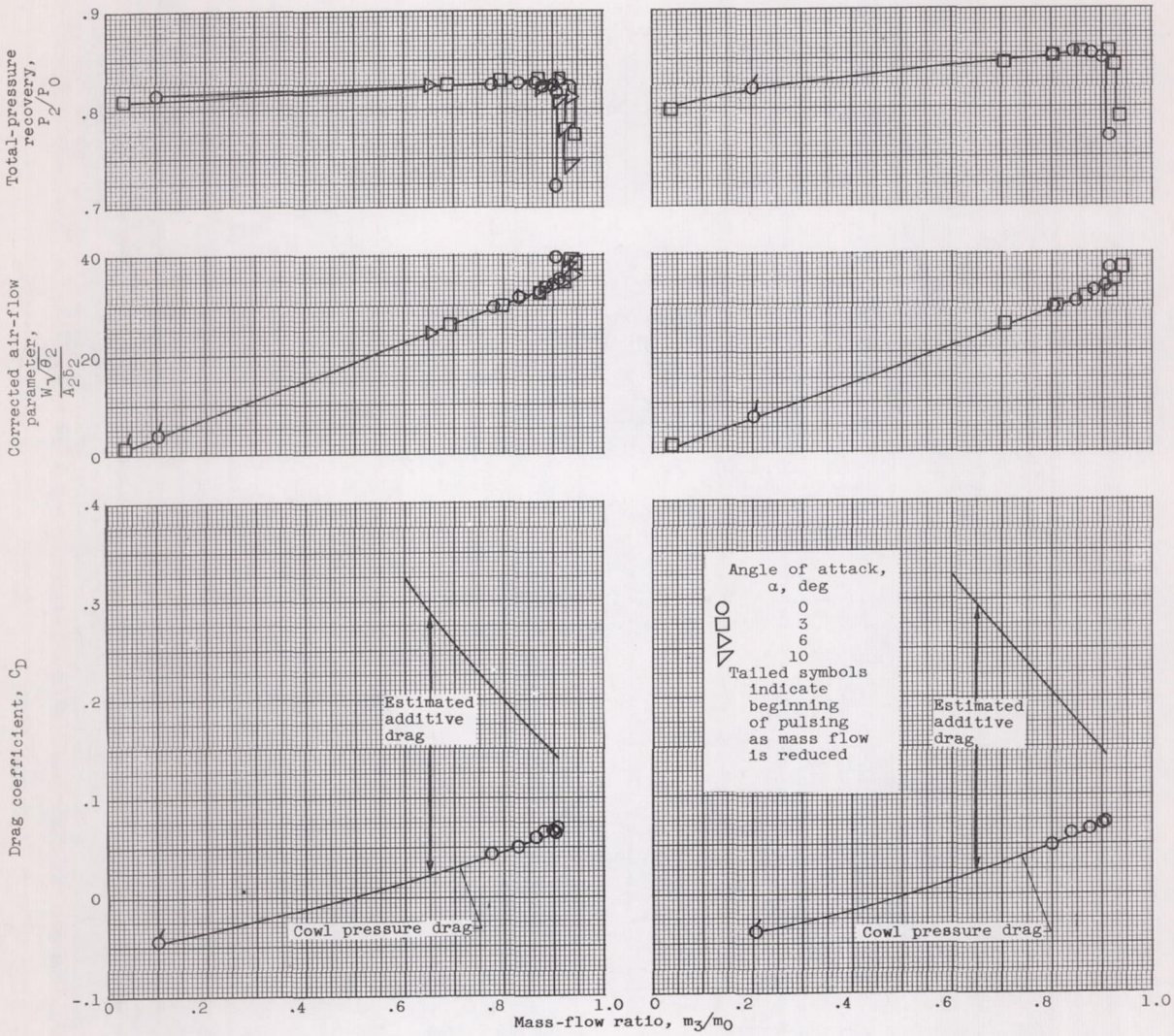

(a) Cowl-position parameter, θ_l, 57°. (b) Cowl-position parameter, θ_l, 48.6°.

Figure 4. - Performance of sharp-lip inlet at free-stream Mach number of 1.8. Shock angle, 46.3°.

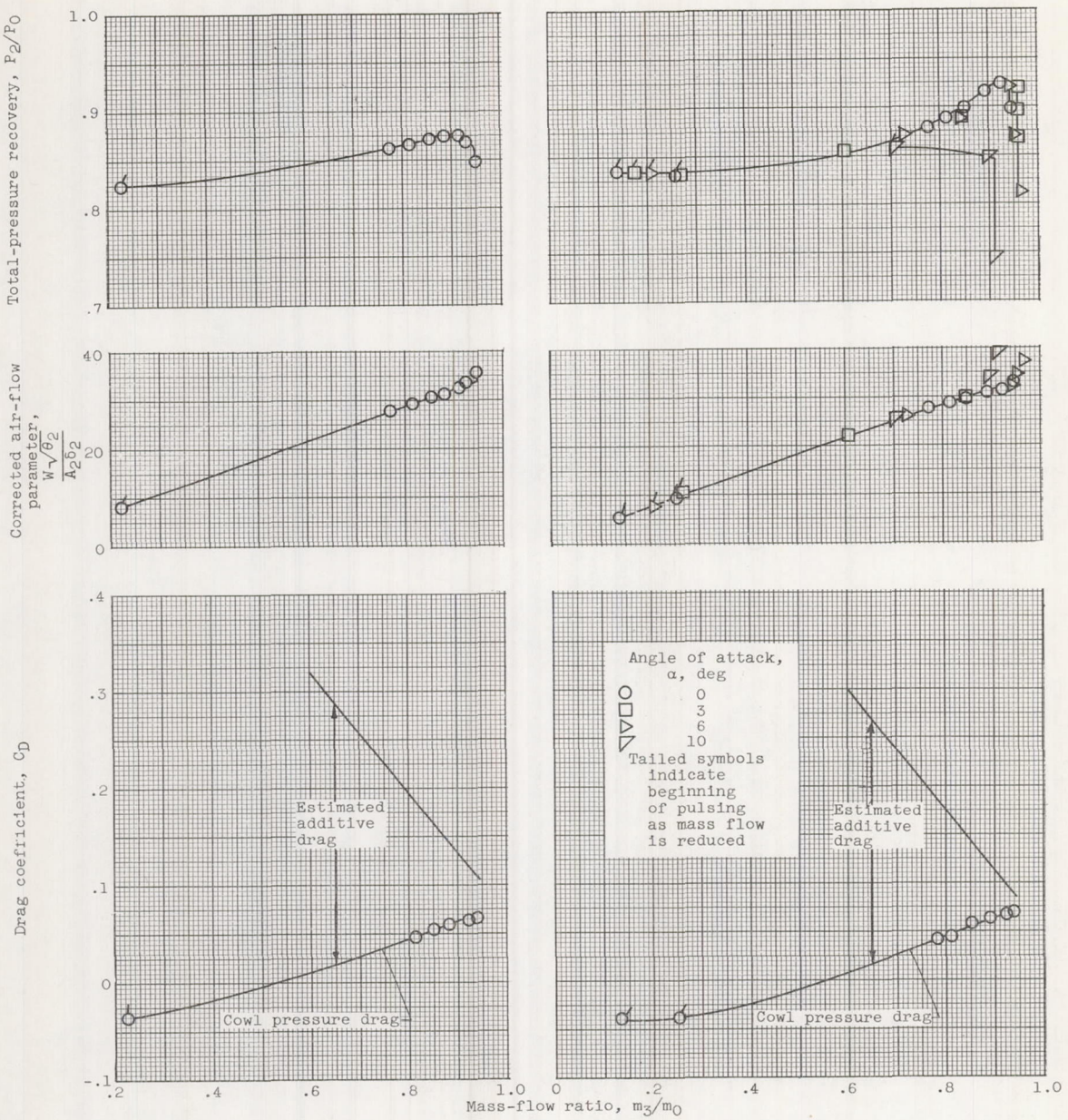

(c) Cowl-position parameter, θ_l, 46.8°.

(d) Cowl-position parameter, θ_l, 44.3°.

Figure 4. - Continued. Performance of sharp-lip inlet at free-stream Mach number of 1.8. Shock angle, 46.3°.

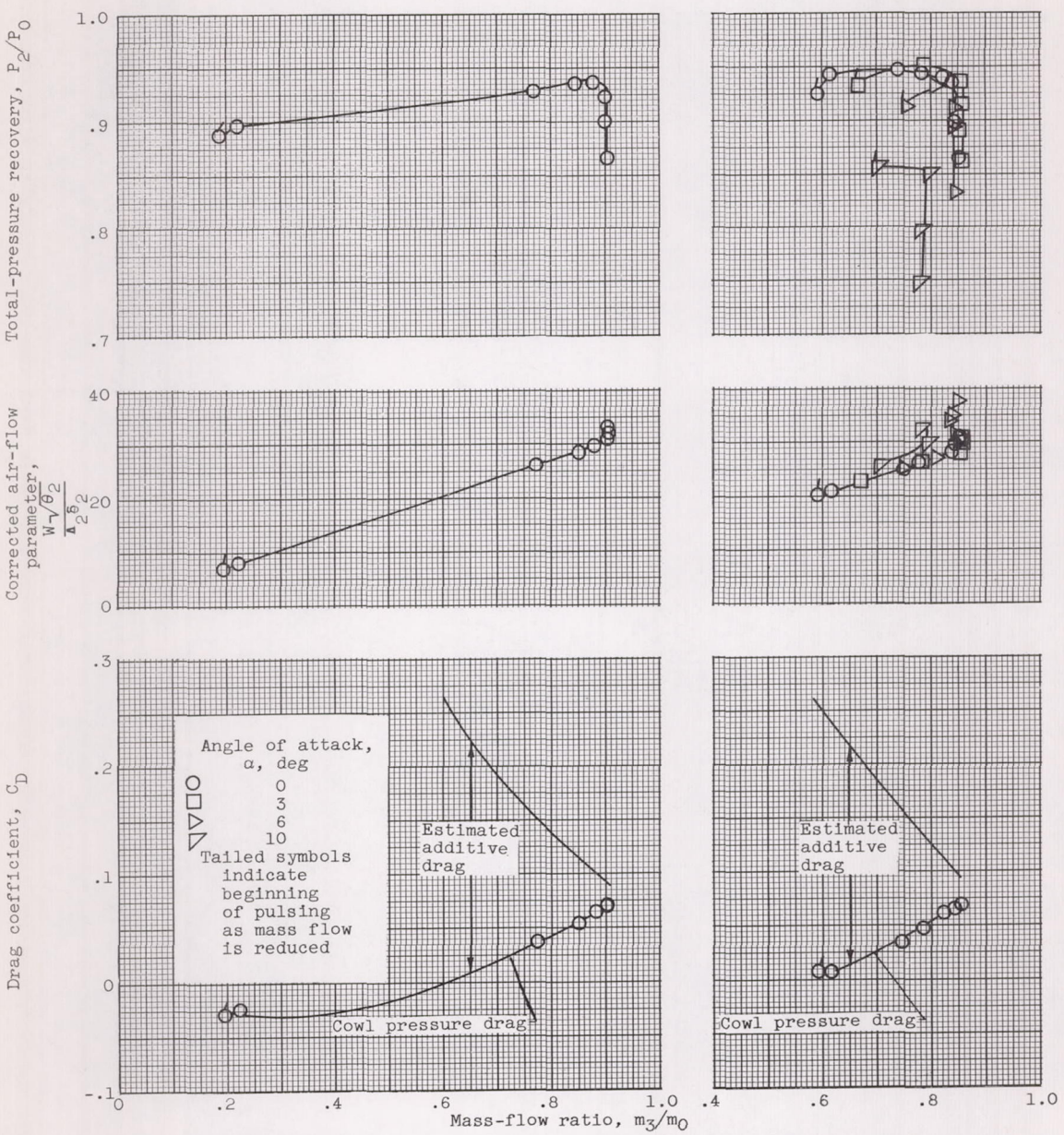

(e) Cowl-position parameter, θ_l, 42.1°.

(f) Cowl-position parameter, θ_l, 39.7°.

Figure 4. - Concluded. Performance of sharp-lip inlet at free-stream Mach number of 1.8. Shock angle, 46.3°.

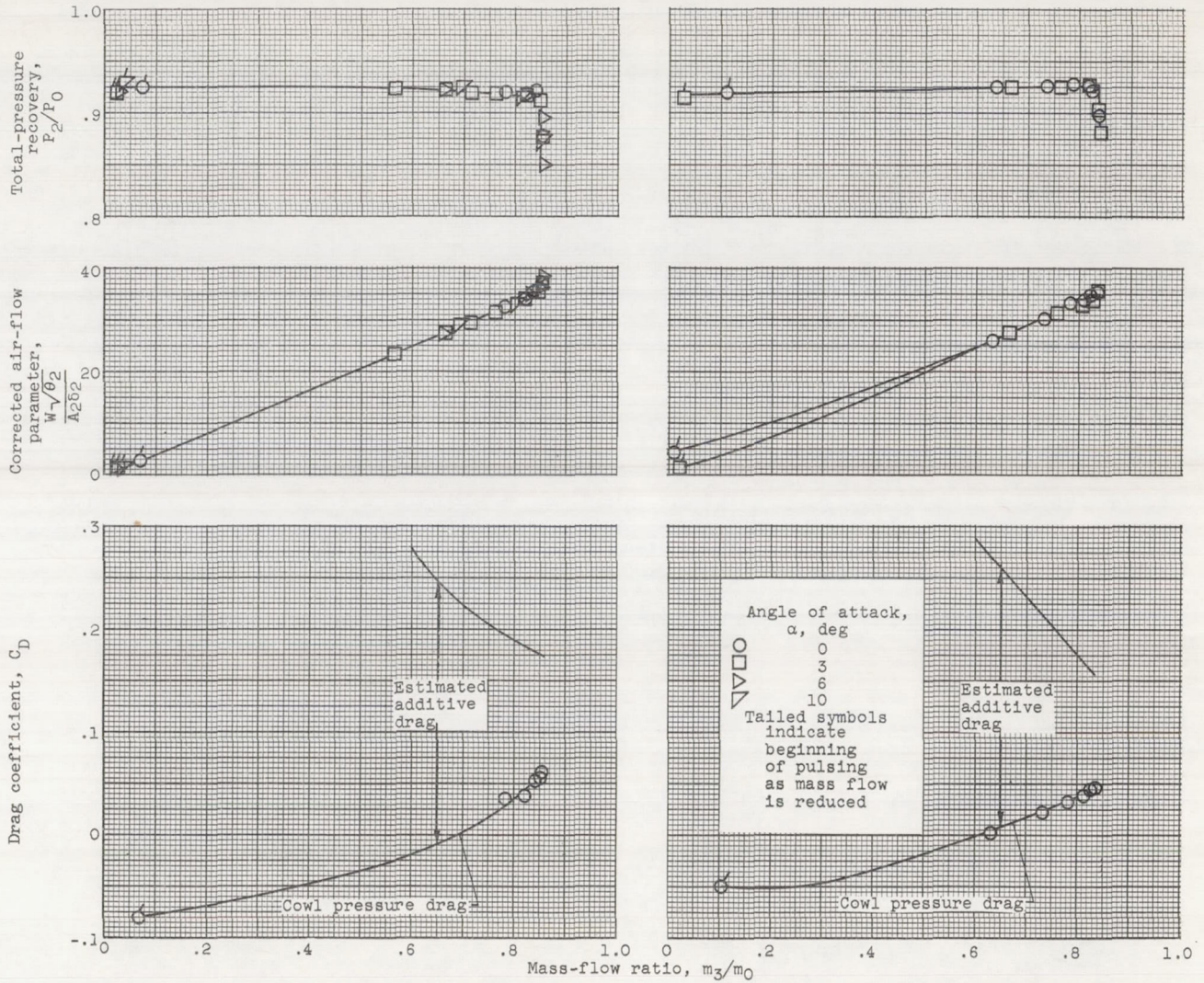

(a) Cowl-position parameter, θ_l, 57°.

(b) Cowl-position parameter, θ_l, 51.9°.

Figure 5. - Performance of sharp-lip inlet at free-stream Mach number of 1.5. Shock angle, 55.0°

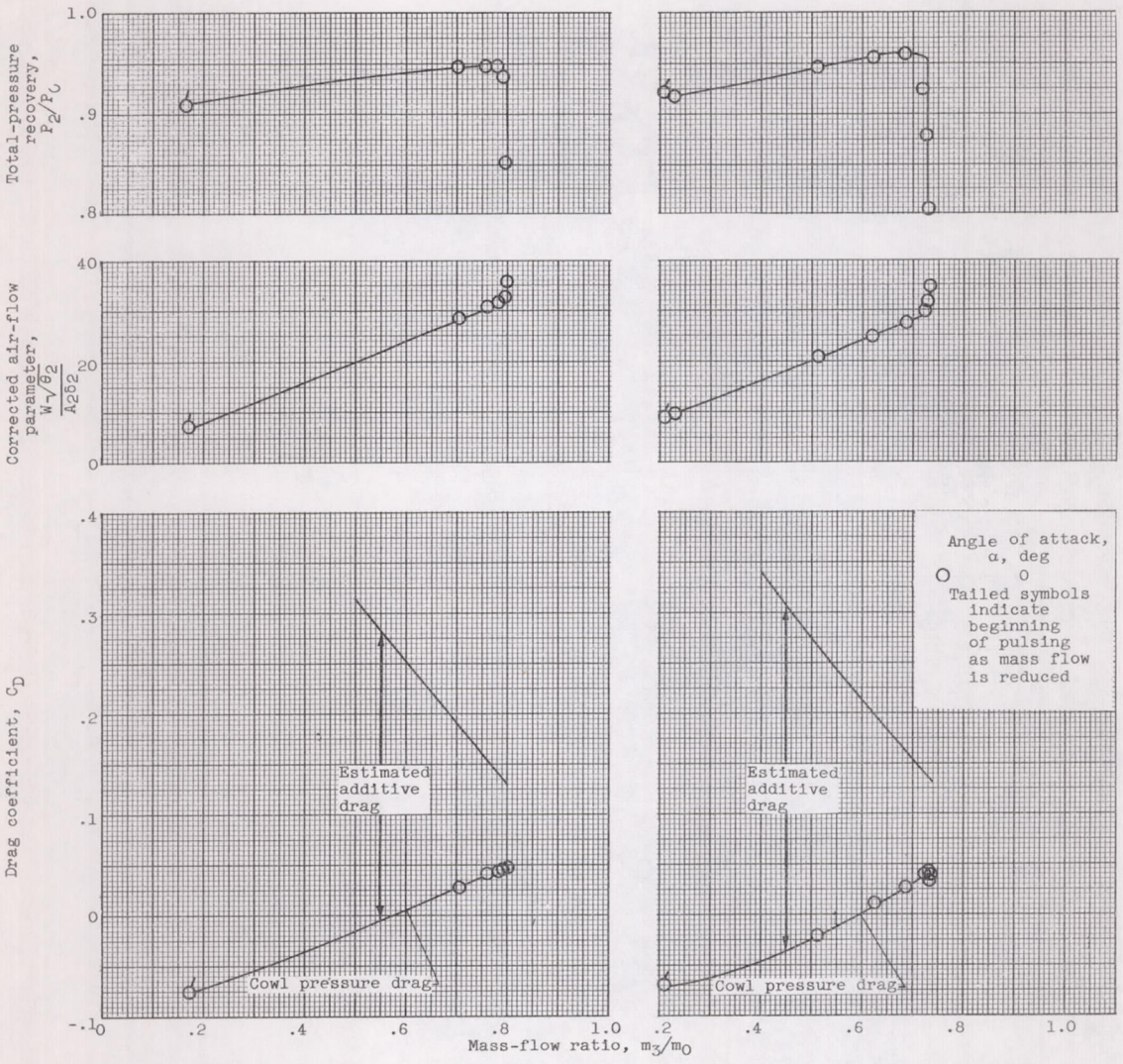

(c) Cowl-position parameter, θ_l, 44.3°.

(d) Cowl-position parameter, θ_l, 40.8°.

Figure 5. - Continued. Performance of sharp-lip inlet at free-stream Mach number of 1.5. Shock angle, 55.0°.

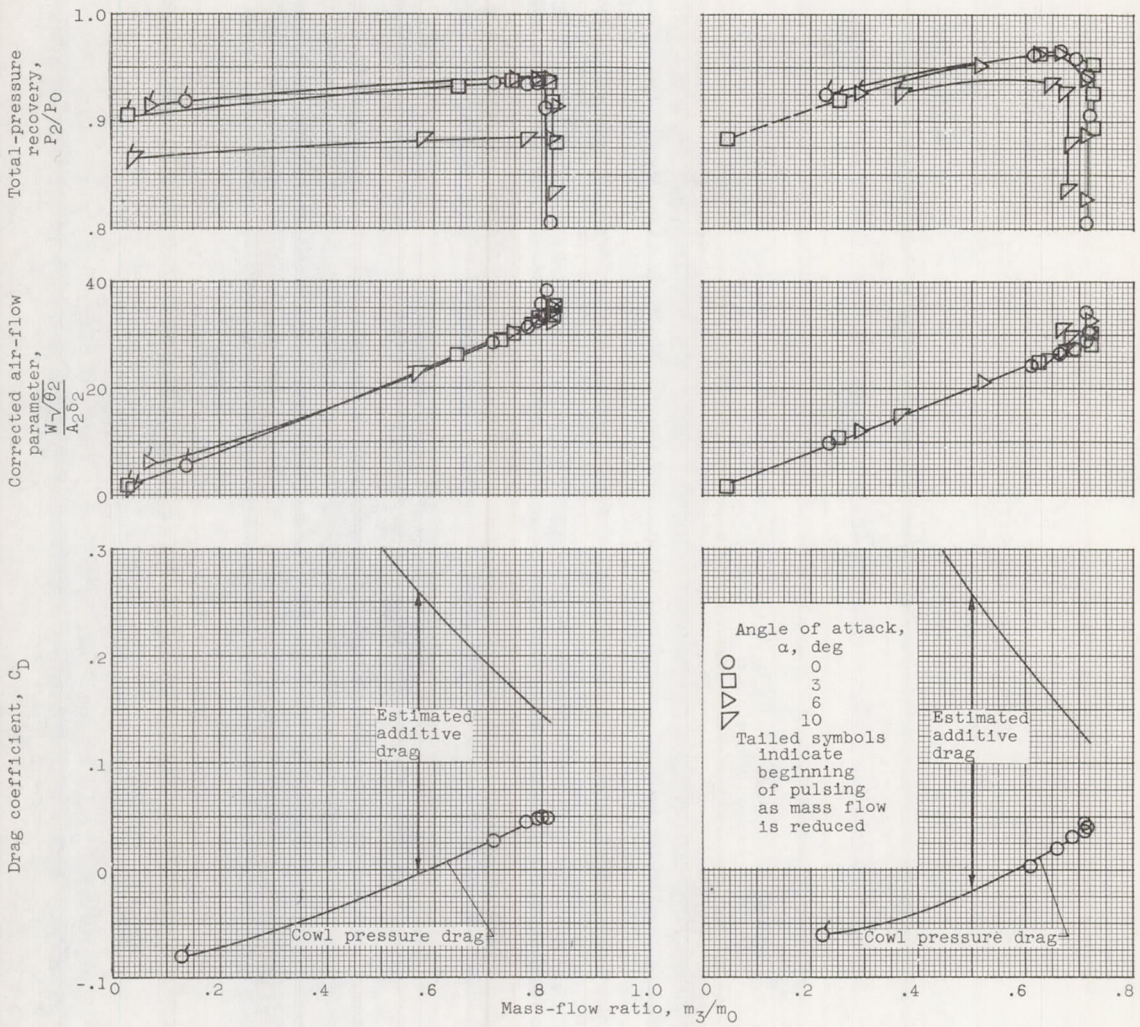

(e) Cowl-position parameter, θ_l, 46.8°. (f) Cowl-position parameter, θ_l, 39.7°.

Figure 5. - Concluded. Performance of sharp-lip inlet at free-stream Mach number of 1.5. Shock angle, 55.0°.

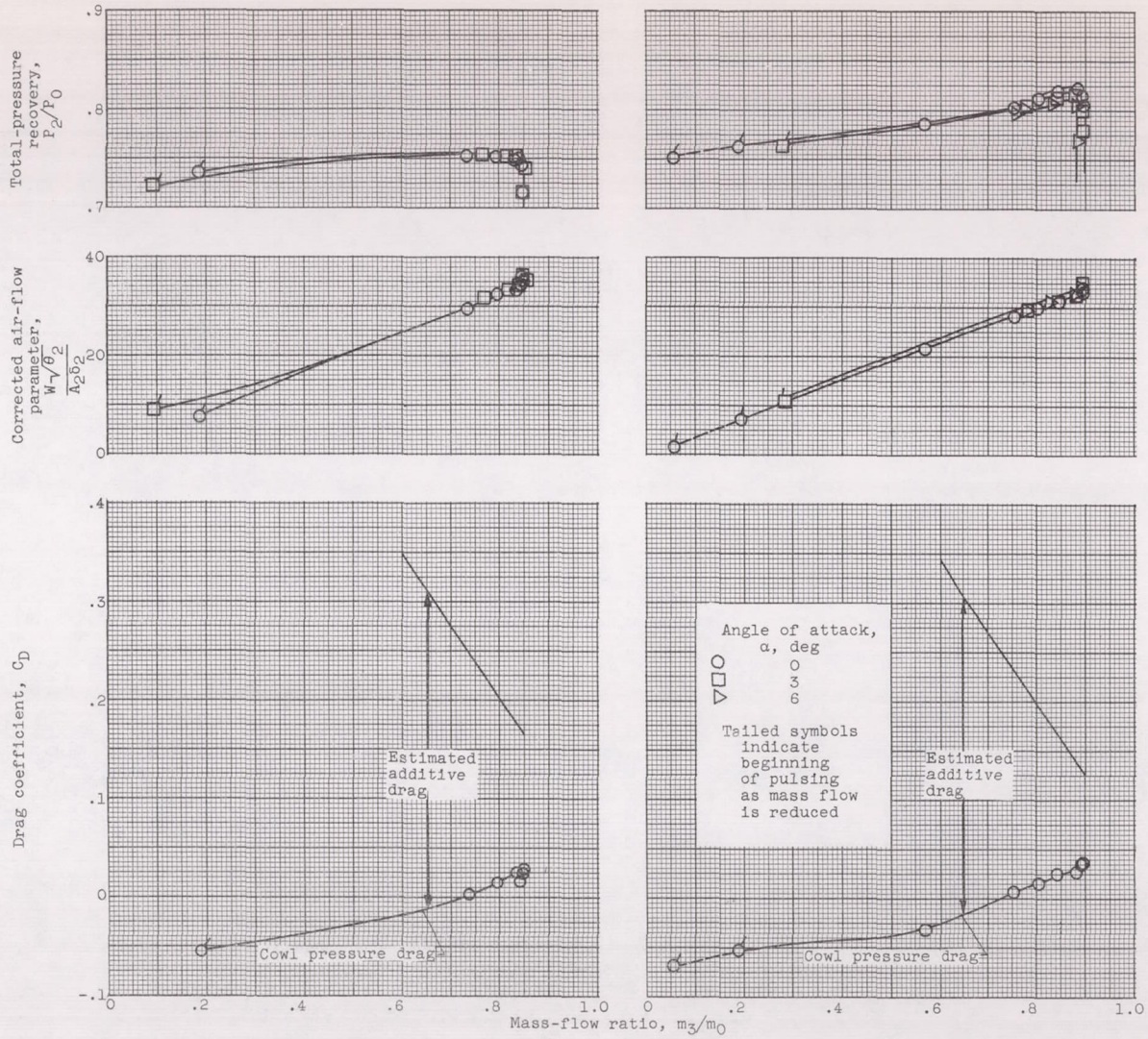

(a) Cowl-position parameter, θ_l, 51.6°.

(b) Cowl-position parameter, θ_l, 42.9°.

Figure 6. - Performance of blunt-lip inlet at free-stream Mach number of 2.0. Shock angle, 43.0°.

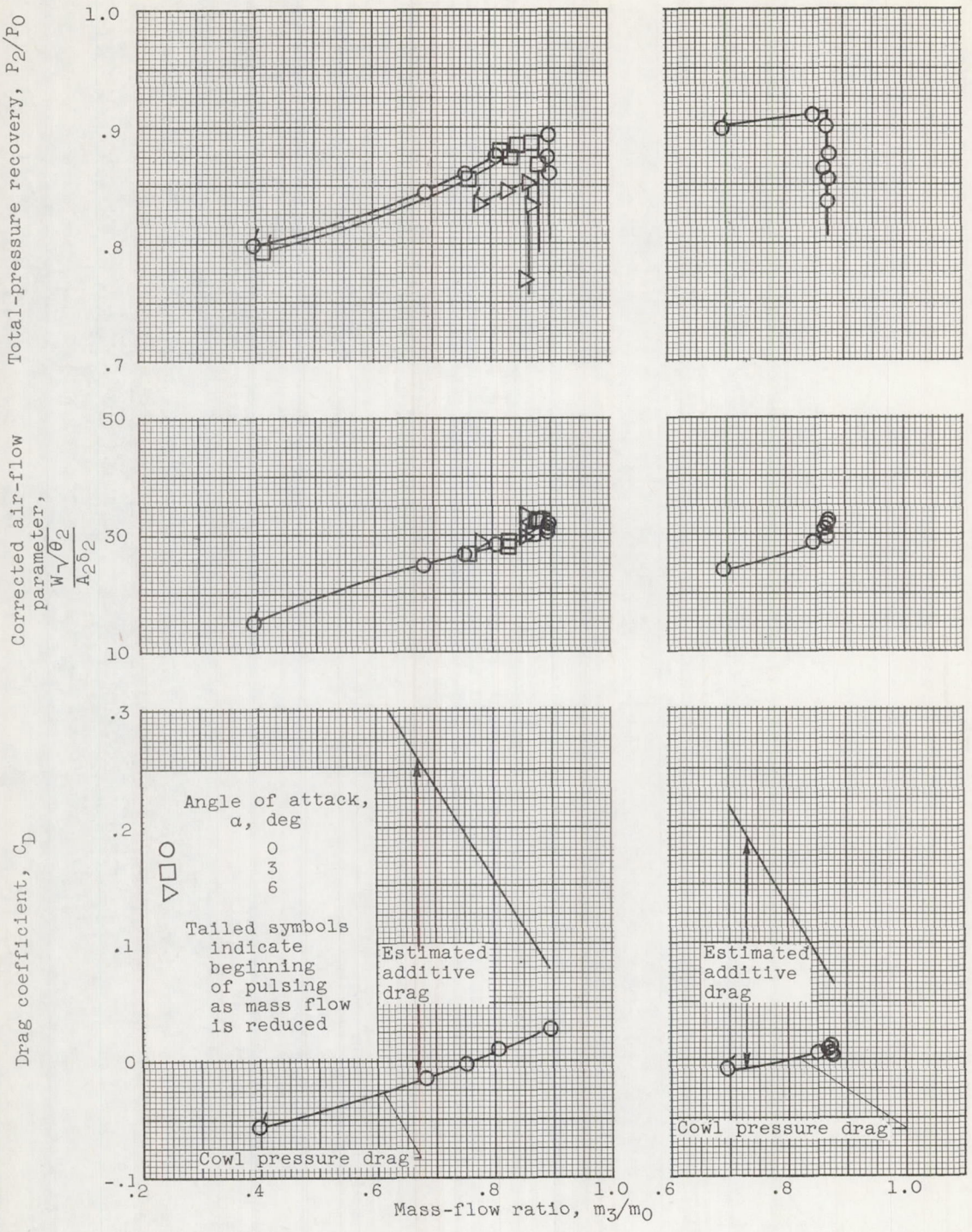

(c) Cowl-position parameter, θ_l, 40.6°.

(d) Cowl-position parameter, θ_l, 39.5°.

Figure 6. - Continued. Performance of blunt-lip inlet at free-stream Mach number of 2.0. Shock angle, 43.0°.

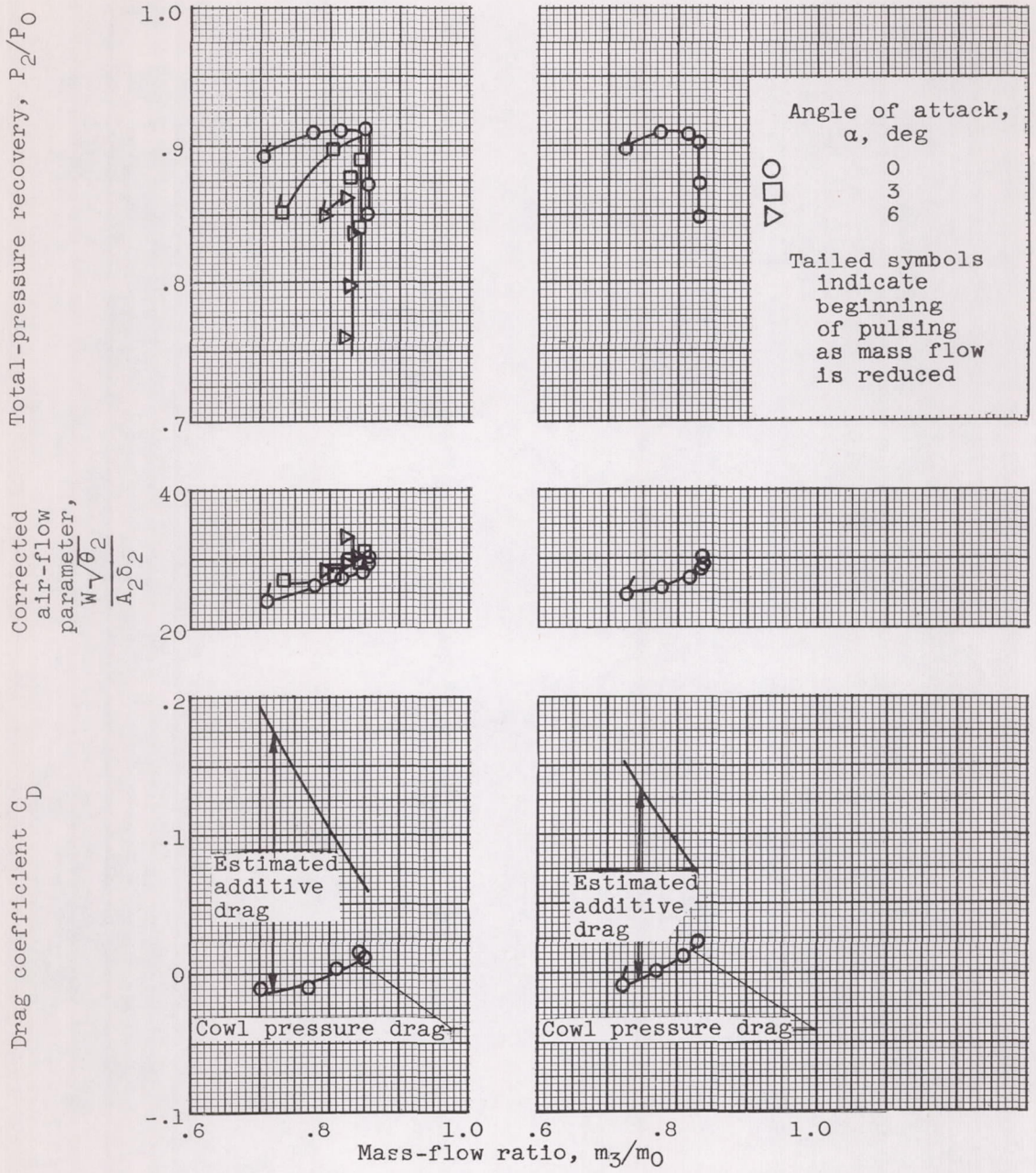

(e) Cowl-position parameter, θ_l, 38.5°.

(f) Cowl-position parameter, θ_l, 37.5°.

Figure 6. - Concluded. Performance of blunt-lip inlet at free-stream Mach number of 2.0. Shock angle, 43.0°.

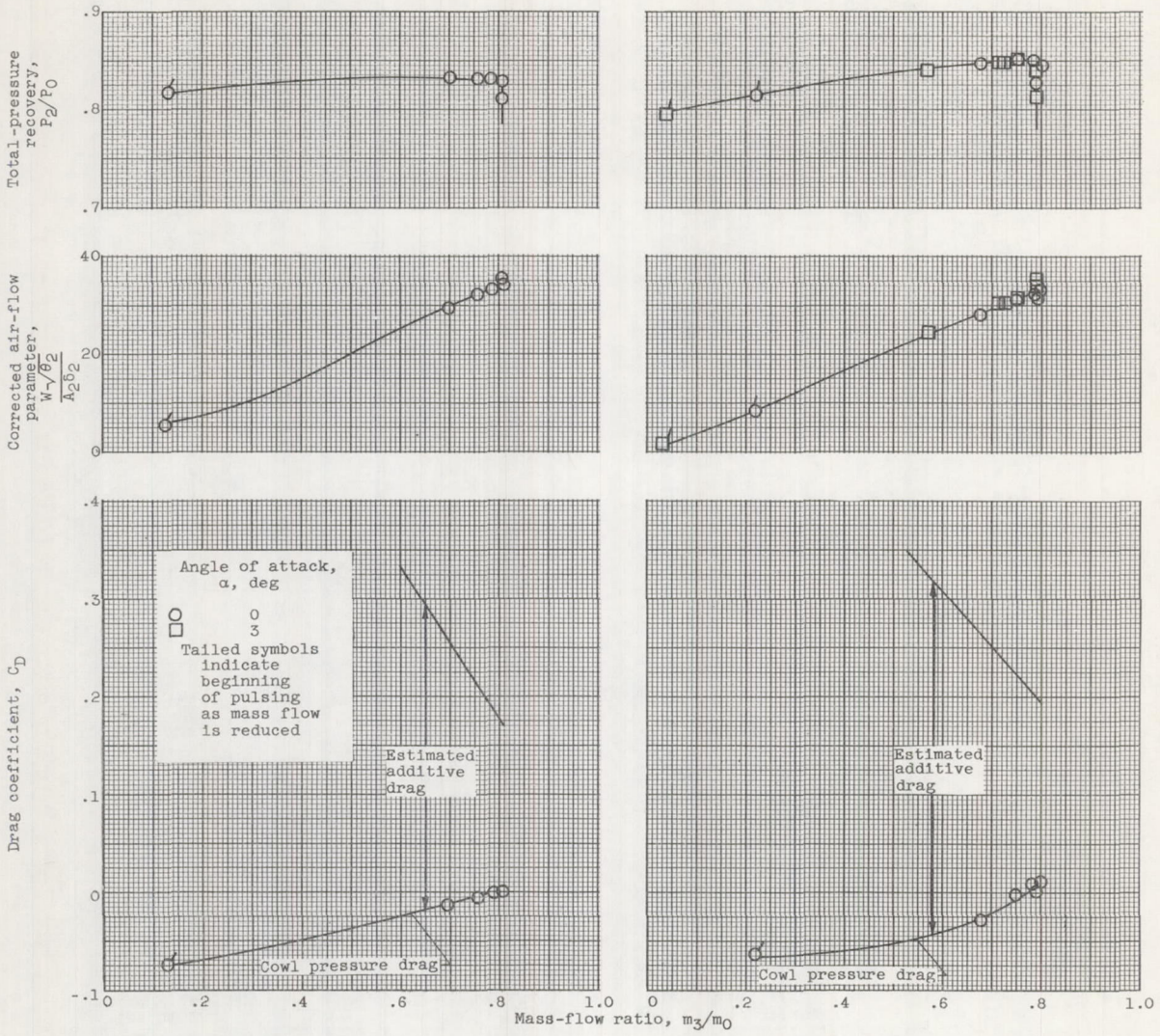

(a) Cowl-position parameter, θ_l, 51.6°. (b) Cowl-position parameter, θ_l, 46.9°.

Figure 7. - Performance of blunt-lip inlet at free-stream Mach number of 1.8. Shock angle, 46.3°.

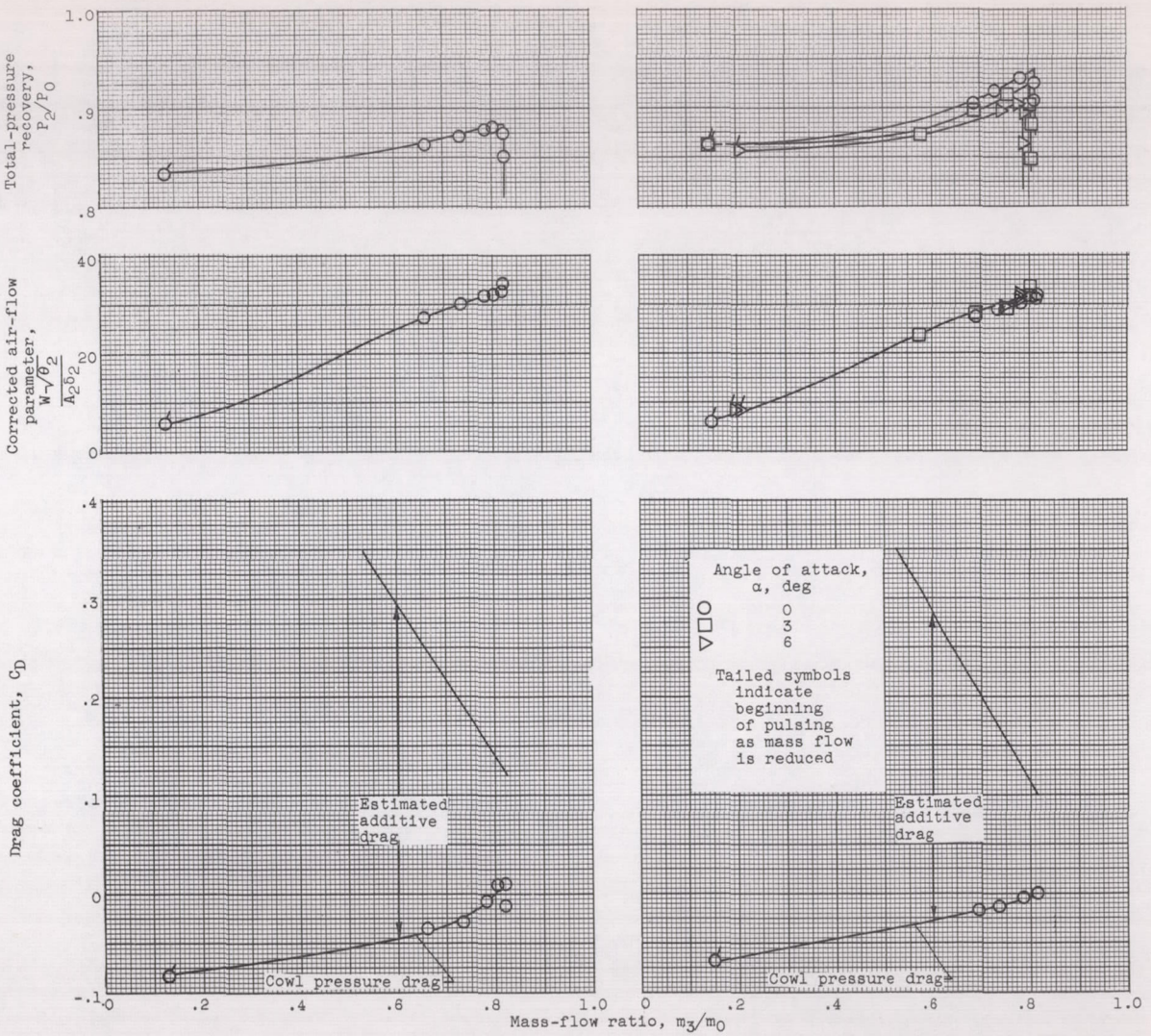

(c) Cowl-position parameter, θ_l, 43.7°.

(d) Cowl-position parameter, θ_l, 41.4°.

Figure 7. - Continued. Performance of blunt-lip inlet at free-stream Mach number of 1.8. Shock angle, 46.3°.

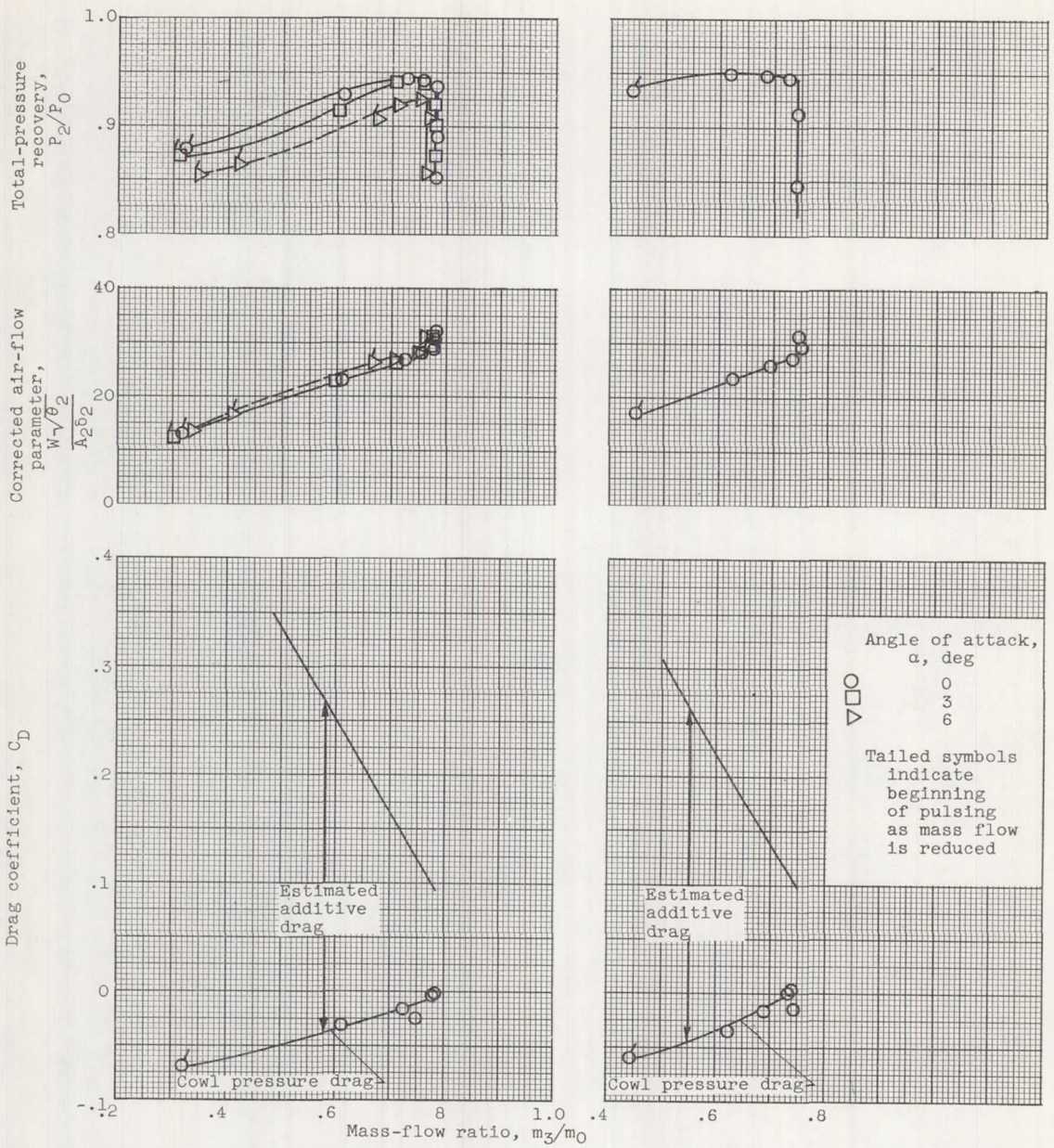

(e) Cowl-position parameter, θ_l, 39.5°. (f) Cowl-position parameter, θ_l, 37.5°.

Figure 7. - Concluded. Performance of blunt-lip inlet at free-stream Mach number of 1.8. Shock angle, 46.3°.

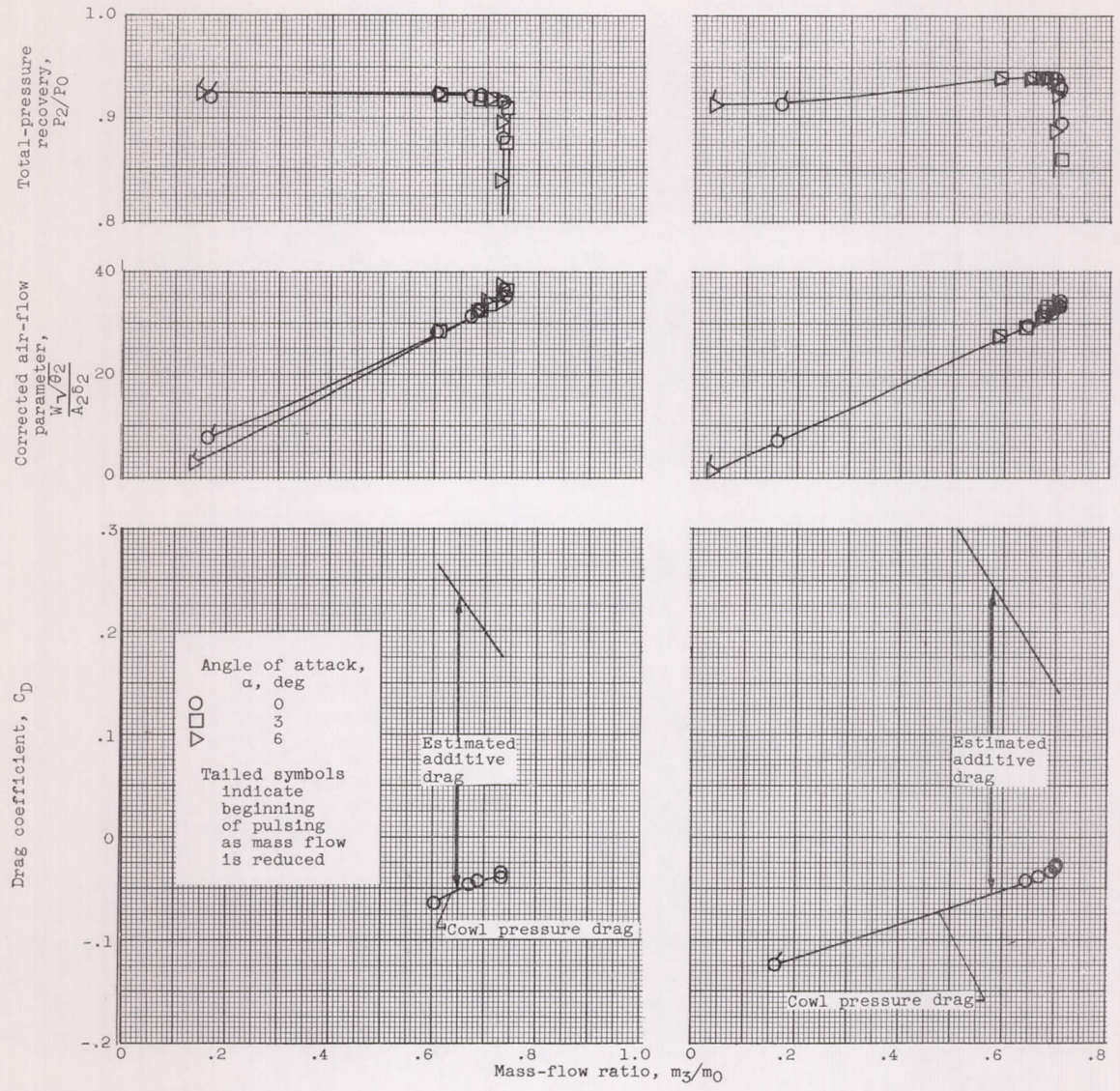

(a) Cowl-position parameter, θ_l, 51.6°. (b) Cowl-position parameter, θ_l, 43.7°.

Figure 8. - Performance of blunt-lip inlet at free-stream Mach number of 1.5. Shock angle, 55.0°.

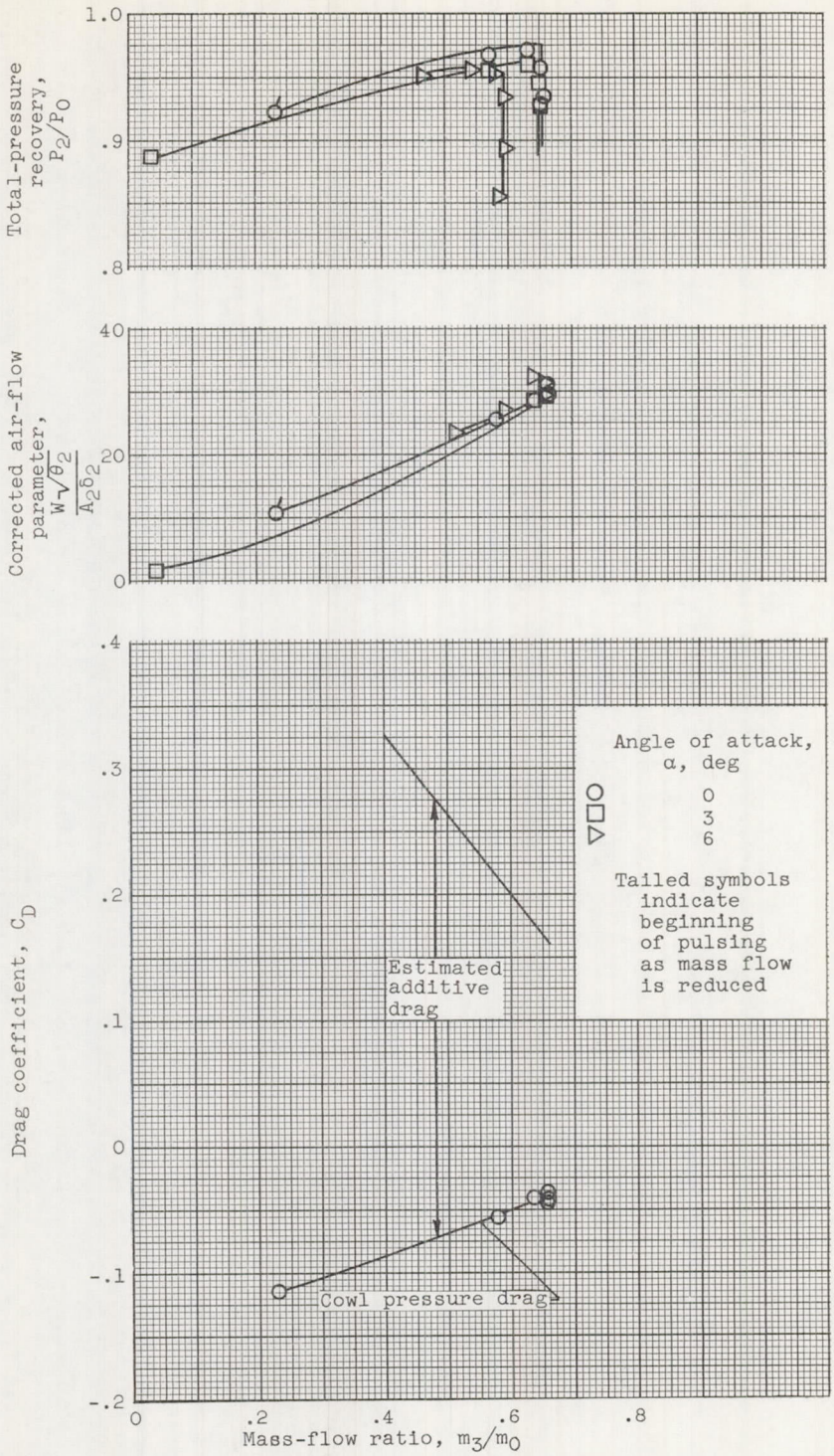

(c) Cowl-position parameter, θ_l, 39.5°.

Figure 8. - Concluded. Performance of blunt-lip inlet at free-stream Mach number of 1.5. Shock angle, 55.0°.

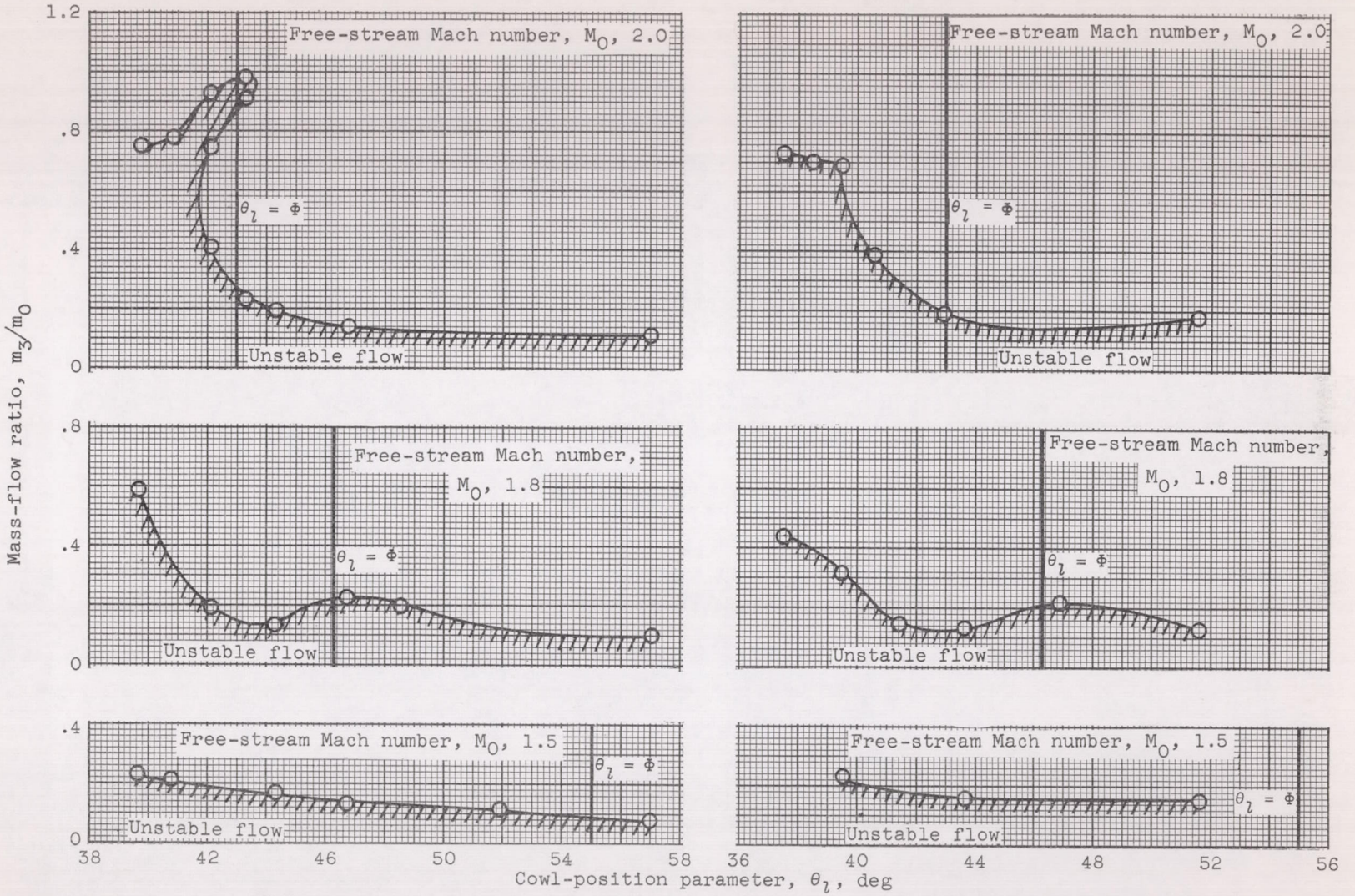

(a) Sharp-lip cowl.

(b) Blunt-lip cowl.

Figure 9. - Effect of spike translation on stability range at zero angle of attack.

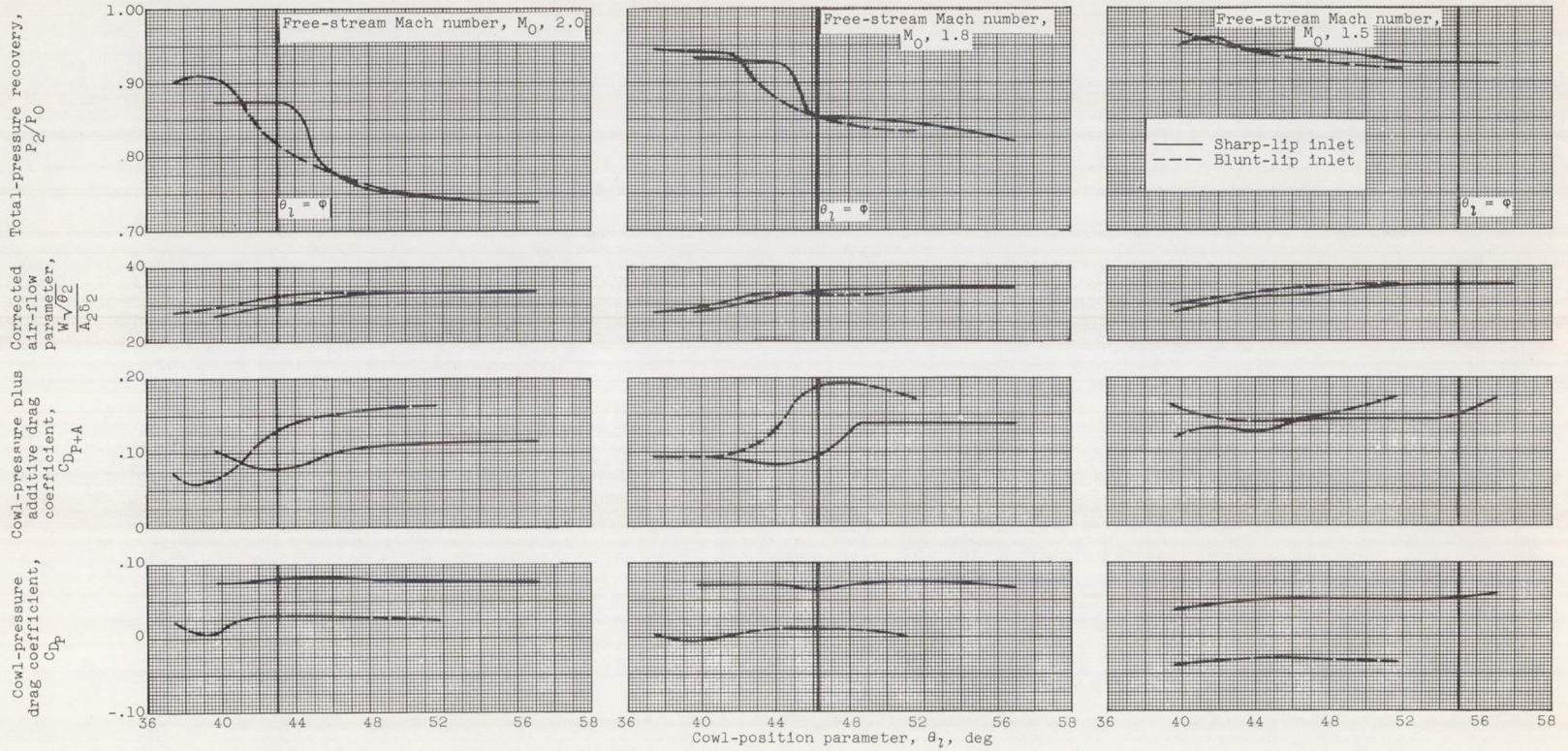

Figure 10. - Effect of spike translation on inlet characteristics at critical operation and zero angle of attack.

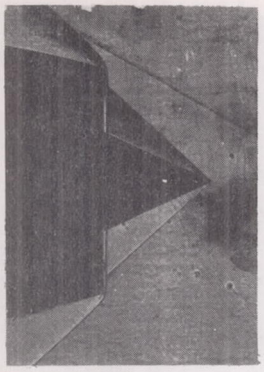

(1) $M_0 = 2.0$; $\theta_l^0 = 46.8$.

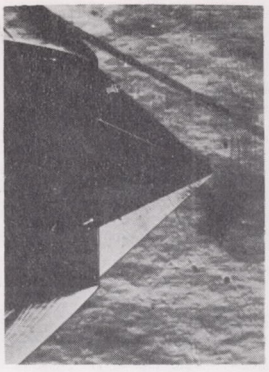

(2) $M_0 = 2.0$; $\theta_l^0 = 44.3$.

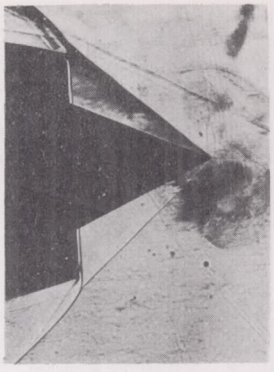

(3) $M_0 = 2.0$; $\theta_l^0 = 39.7$.

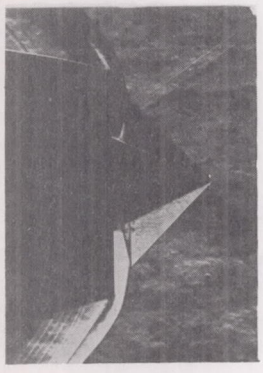

(4) $M_0 = 1.8$; $\theta_l^0 = 48.6$.

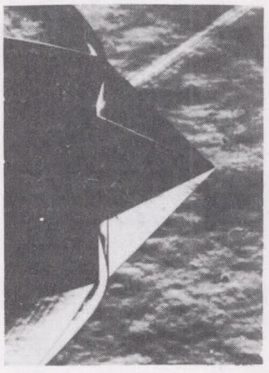

(5) $M_0 = 1.8$; $\theta_l^0 = 44.3$.

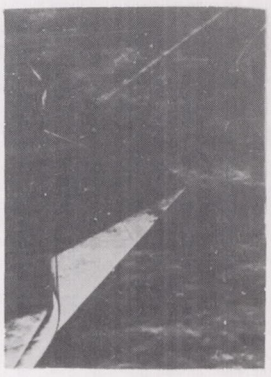

(6) $M_0 = 1.8$; $\theta_l^0 = 39.7$.

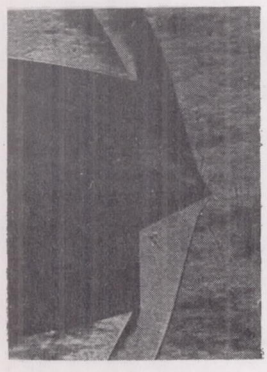

(7) $M_0 = 1.5$; $\theta_l^0 = 57$.

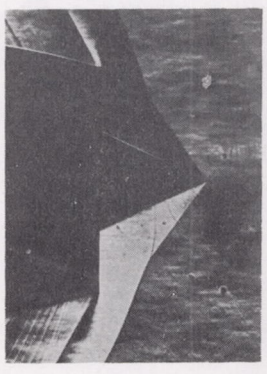

(8) $M_0 = 1.5$; $\theta_l^0 = 46.8$.

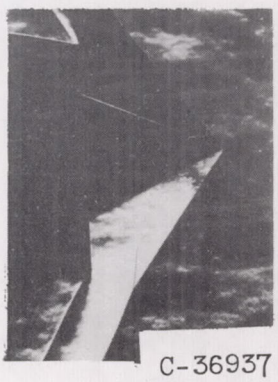

C-36937

(9) $M_0 = 1.5$; $\theta_l^0 = 39.7$.

(a) Sharp-lip inlets.

Figure 11. - Schlieren photographs of translating-spike inlet for various spike positions at critical operation and zero angle of attack.

(1) $M_0 = 2.0$; $\theta_l^0 = 51.6$.

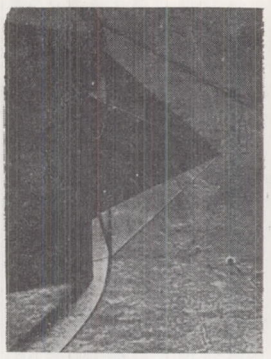

(2) $M_0 = 2.0$; $\theta_l^0 = 42.9$.

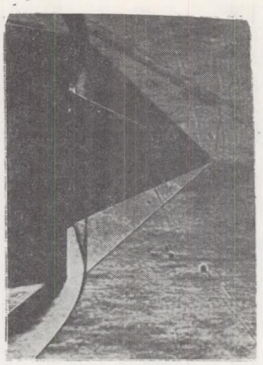

(3) $M_0 = 2.0$; $\theta_l^0 = 39.5$.

(4) $M_0 = 1.8$; $\theta_l^0 = 51.6$.

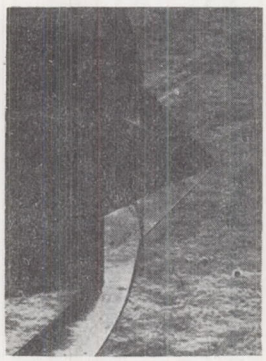

(5) $M_0 = 1.8$; $\theta_l^0 = 46.9$.

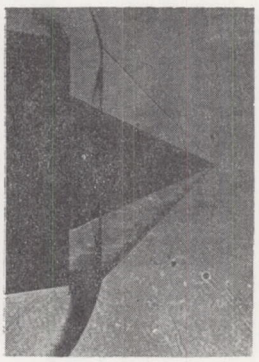

(6) $M_0 = 1.8$; $\theta_l^0 = 39.5$.

(7) $M_0 = 1.5$; $\theta_l^0 = 51.6$.

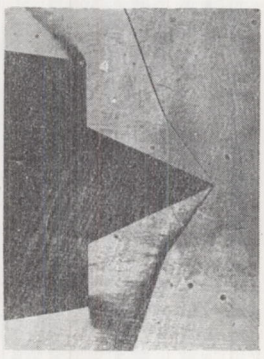

(8) $M_0 = 1.5$; $\theta_l = 43.7$.

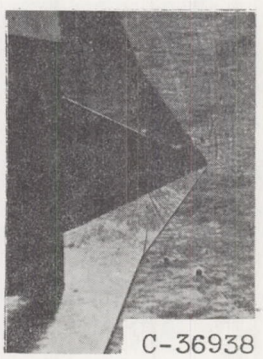

(9) $M_0 = 1.5$; $\theta_l^0 = 39.5$.

(b) Blunt-lip inlet.

Figure 11. - Concluded. Schlieren photographs of translating-spike inlet for various spike positions at critical operation and zero angle of attack.

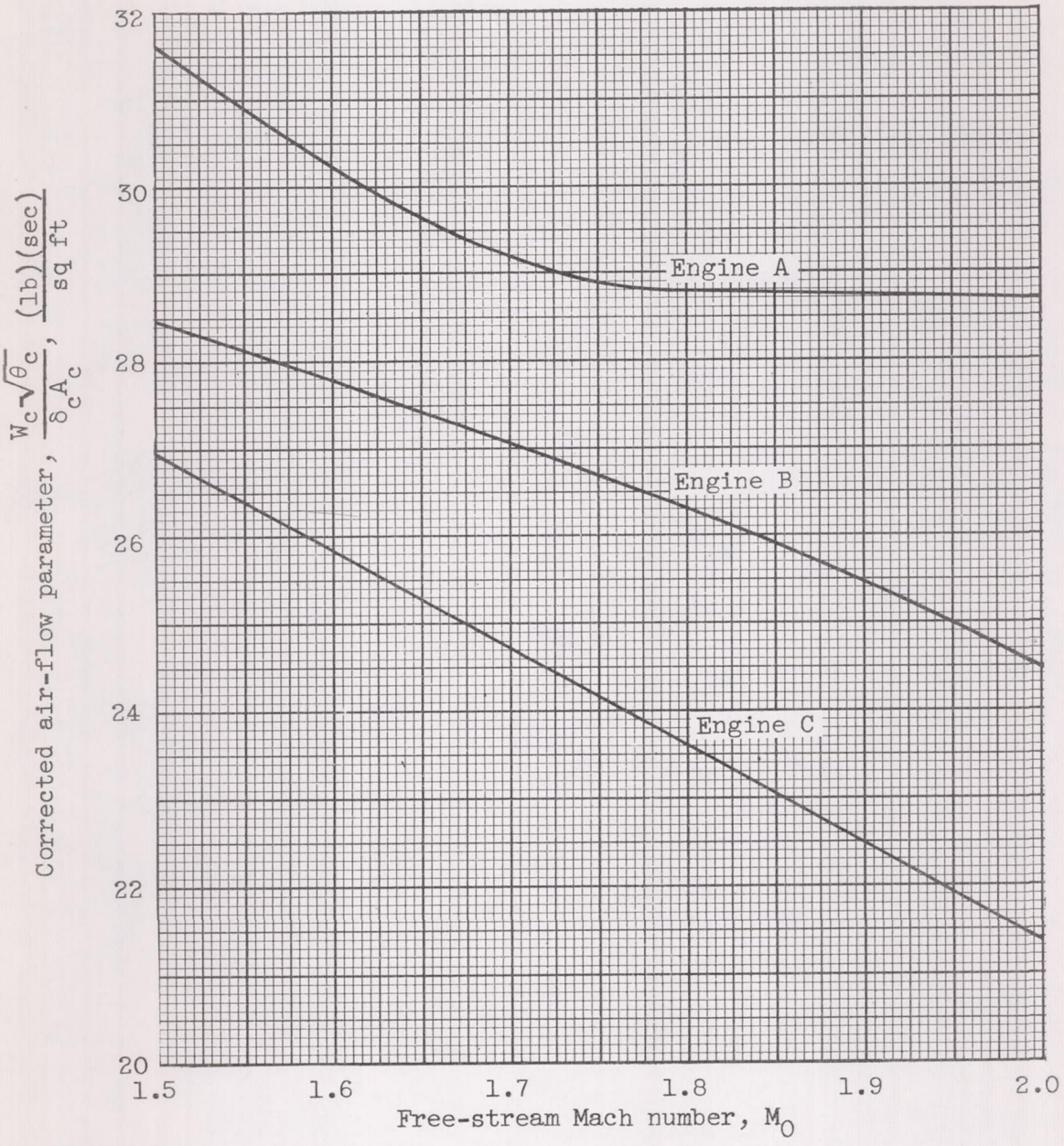

Figure 12. - Schedule of required corrected weight flow for several turbojet engines in speed range of Mach number 1.5 to 2.0. Altitude, 36,000 feet or greater.

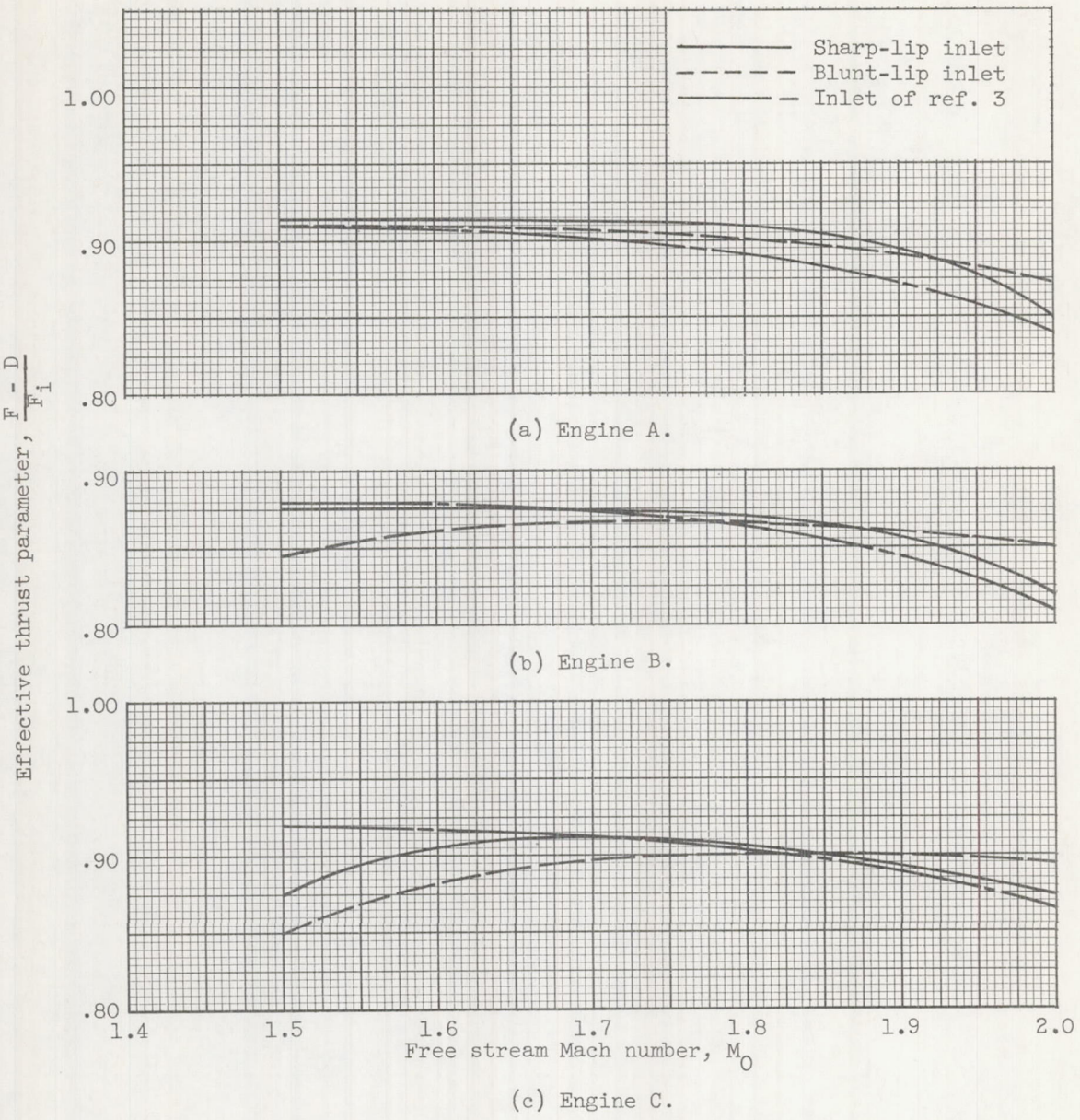

Figure 13. - Performance of several turbojet engines matched with differently designed translating-spike inlets. Altitude, 35,000 feet or greater.

3497

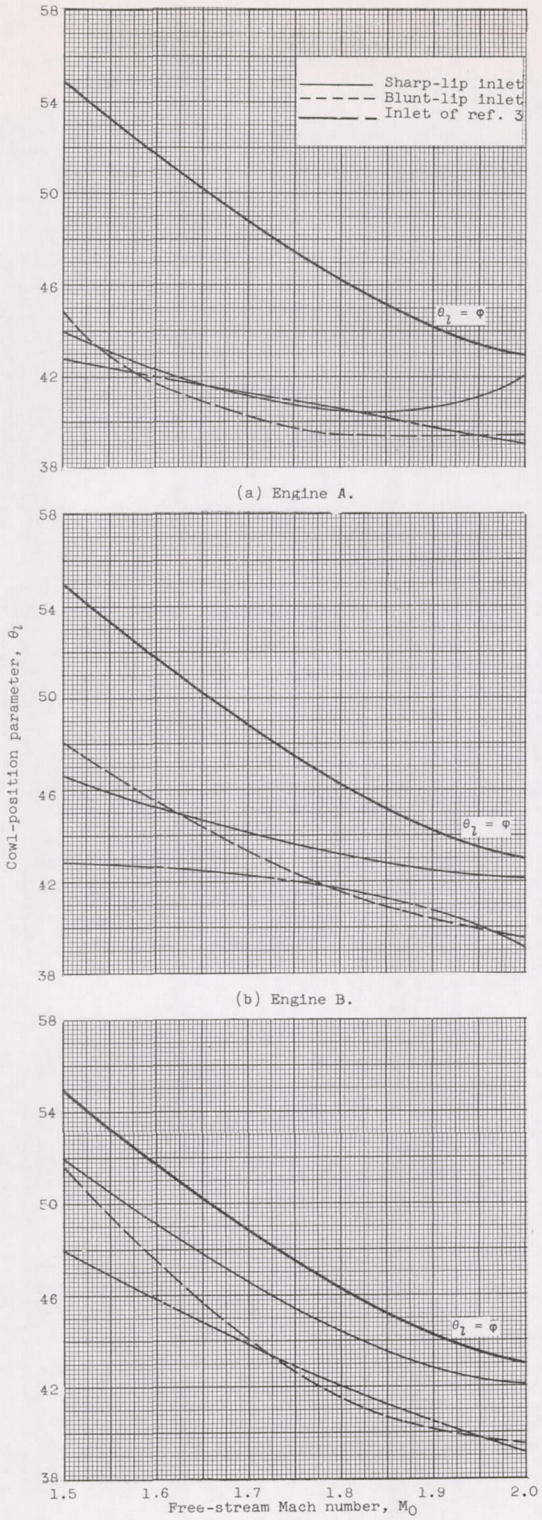

(a) Engine A.

(b) Engine B.

(c) Engine C.

Figure 14. - Schedule of cowl-position parameters for optimized inlet-engine matching. (Inlet sized for optimum performance at free-stream Mach number of 2.0.)